International Journal of Engineering Science 48 (2010) 529–549

Contents lists available at ScienceDirect

International Journal of Engineering Science

journal homepage: www.elsevier.com/locate/ijengsci

Magnetoelastic stresses in a three-phase composite cylinder subject to a uniform magnetic induction

Chun-Bo Lin [a,*], Jui-Lin Lee [b], Shin-Cheng Chen [b]

[a] Department of Industrial Engineering and Management, Overseas Chinese University, Taichung 407, Taiwan, ROC
[b] Department of Automation Engineering, Nan Kai University of Technology, Nantou 542, Taiwan, ROC

ARTICLE INFO

Article history:
Received 13 August 2009
Received in revised form 24 December 2009
Accepted 1 January 2010
Available online 1 February 2010

Communicated by M. Kachanov

Keywords:
Magnetoelastic stress
Alternating technique
Three-phase composite cylinder

ABSTRACT

A solution of magnetoelastic stresses on a three-phase composite cylinder subjected to a remote uniform magnetic induction is derived in this study. Based upon the complex variable theory and the method of analytical continuation together with alternating technique, the general expressions of both the magnetic and the magnetoelastic field quantities can be obtained. The variations of the magnetoelastic stress on various parameters are displayed in graphic form. Comparisons between the results of this work and the existing solutions in literature under special cases reveal that the present solution is correct and general.

1. Introduction

In the past few decades, the use of composite materials in engineering application increases rapidly. Therefore, the stress analysis of layered media has been investigated by earlier researchers. Due to the necessity in considering the boundary conditions on each of the multiple interfaces for such a problem, the solving process becomes more complicated as comparing with the homogeneous counterpart. Thus the stress analysis of multi-layered media problem results in finding the solution for a system of simultaneous equations with a lot of unknown constants as derived by Iyengar and Alwar [1] and Chen [2]. Nevertheless, several methods have been developed to provide an efficient approach in studying the elastic problem of multi-layered media. Such as Bulfer [3] used the method of transfer matrix which is expressed in terms of the infinite series expansion and can be solved with various orders of approximation, Lin and Keer [4] applied the flexibility matrix approach with the boundary integral formulation to solve the elastic problem of a vertical crack in a multi-layered medium. Based upon the alternating technique, Choi and Earmme [5] conducted the stress analysis of the singularity problem in an isotropic plane layered trimaterial. Comparing with the aforementioned studies of straight interfaces, the corresponding problem of circular interfaces may involve more mathematical complexity. Several investigators considered the elastic problem of a three-phase cylinder. As denoted by Benveniste et al. [6], a three-phase circular boundary problem with perfect interfaces can be transformed into a corresponding two-phase problem with imperfect interface by letting the thickness of intermediate phase tends to zero. Luo [7] employed the Laurent series expansion and the method of analytical continuation to find a solution for the elastic problem of three-phase composite cylinder with an edge dislocation at the intermediate annular region. By the use of heterogenization technique, Honein et al. [8] considered the anti-plane elastostatics of circularly cylindrical and plane layered media. Chao et al. [9] used the alternating technique with analytic continuation to obtain the

* Corresponding author. Present address: 100, Ciao Guang Rd., Taichung 407, Taiwan, ROC. Tel.: +886 4 27016855x1201; fax: +886 4 24527824.
E-mail address: cblin@ocu.edu.tw (C.-B. Lin).

0020-7225/$ - see front matter © 2010 Elsevier Ltd. All rights reserved.
doi:10.1016/j.ijengsci.2010.01.002

stress evoked by a point force. To the authors' knowledge, the magnetoelastic problem of a three-phase cylinder is still a new topic and cannot be found in the literature.

Due to the possible application of a structure in a magnetic environment, the interaction between the magnetic field and the deformation of the structure is a relevant concern. Especially in an environment of strong magnetic field, such as magnetic fusion reactor and magnetic levitated vehicles, the analysis of magnetoelastic interaction is necessary in considering the safety of structure. Just like that in the pure elastic case, the application of composite material is also competent in the magnetoelastic one. For the problem associated with inhomogeneities in magnetoelasticity, Maugin et al. [10] presented a theoretic formulation of nonlinear anisotropic inhomogeneous electromagnetoelasticity. Lin [11] used the technique of conformal mapping and the method of analytical continuation to find the magnetic and the magnetoelastic fields on both the matrix and a perfectly bonded elliptic inclusion. Based upon the complex variable theory and the method of analytical continuation, Lin and Chen [12] found the magnetoelastic stresses on a circular shell subjected to a point magnetic source or a remote uniform magnetic induction. By applying the Laurent series expansion and expanding the definition of Airy's stress function to magnetoelasticity, Chen and Lin [13] obtained the magnetoelastic fields for an infinite matrix with multiple circular inclusions.

In this study, we applied the formulation of magnetoelasticity in complex variable form and the alternating technique to derive the magnetic field and the magnetoelastic field in a three-phase composite cylinder under a remote uniform magnetic induction. The distributions of magnetoelastic stress are displayed graphically and the results of this study are compared with the previous studies under special cases.

2. Magnetic field

The magnetic induction can be expressed in terms of a complex potential function as

$$B_x + \mathrm{i}B_y = \mu_0\mu_r(H_x + \mathrm{i}H_y) = \mu_0\mu_r\overline{h'(z)} \tag{1}$$

where B_i and H_k denote magnetic induction (or magnetic flux density) and magnetic intensity; $\mu_0 = 4\pi\times10^{-7}$ newton/ampere^2 is a universal constant and μ_r is relative magnetic permeability. The complex potential function $h(z)$ of magnetic field is an analytic function in terms of the complex variable $z = x + \mathrm{i}y$ and can be represented as

$$h(z) = \varphi(x,y) + \mathrm{i}\gamma(x,y) \tag{2}$$

where $\varphi(x, y)$ and $\gamma(x, y)$ denote the real and the imaginary parts of $h(z)$. With the integration along the boundary of a body,

$$\begin{aligned}
&\int (H_x dx + H_y dy) = \int \left(\frac{\partial\varphi}{\partial x}dx + \frac{\partial\varphi}{\partial y}dy\right) = \varphi,\\
&\int (B_x n_x + B_y n_y)ds = \int \left(B_x\frac{dy}{ds} - B_y\frac{dx}{ds}\right)ds = \int \mu_0\mu_r\left(\frac{\partial\gamma}{\partial y}dy + \frac{\partial\gamma}{\partial x}dx\right) = \mu_0\mu_r\gamma
\end{aligned} \tag{3}$$

the boundary conditions can be described as the continuation of φ and $\mu_0\mu_r\gamma$ across the interface. Consider a composite cylinder with three dissimilar isotropic ferromagnetic materials bonded along two concentric interfaces L and L^*, under a uniform magnetic induction as shown in Fig. 1. Three different materials a, b and c occupy the concentric regions S_a, S_b and S_c, respectively. The magnetic fields on the trimaterial cylinder under a uniform magnetic induction can be found by applying the alternating technique.

Step 1: analytic continuation across the interface L

In the first step, the regions S_a and S_b are regarded to be composed of the same material b and the region S_c is consisted of material c. The magnetic potential function can be represented as

$$h_{1b}(z) = \begin{cases} h_1(z) & z \in S_a \cup S_b \\ h_0(z) + h_{c0}(z) & z \in S_c \end{cases} \tag{4}$$

where the subscript $1b$ in $h_{1b}(z)$ denotes the first time to consider the continuity conditions across the interface L(i.e. $r = b$). The symbol $h_0(z)$ represents the complex potential function of the applied uniform magnetic induction, $h_1(z)$ is holomorphic in the interior region $S_a \cup S_b$ and $h_{c0}(z)$ is holomorphic in the exterior region S_c. Notice that the complex potential function $h_0(z) = (B_0/\mu_0\mu_{rc})e^{-\mathrm{i}\gamma}z$ of the applied magnetic induction is holomorphic in an interior region containing the origin. As shown in Fig. 1, the applied magnetic induction with strength B_0 is assumed to be conducted along the direction having at an angle γ with respect to x_1-axis. Furthermore, the appearance of μ_{rc} is due to that a remote uniform magnetic induction is applied into the exterior region S_c. Applying the boundary conditions of magnetic filed across L, one can obtain

$$h_1(\rho_b) + \overline{h_1(\rho_b)} = h_0(\rho_b) + \overline{h_0(\rho_b)} + h_{c0}(\rho_b) + \overline{h_{c0}(\rho_b)} \tag{5}$$

$$\mu_{rb}\left[h_1(\rho_b) - \overline{h_1(\rho_b)}\right] = \mu_{rc}\left[h_0(\rho_b) - \overline{h_0(\rho_b)} + h_{c0}(\rho_b) - \overline{h_{c0}(\rho_b)}\right] \tag{6}$$

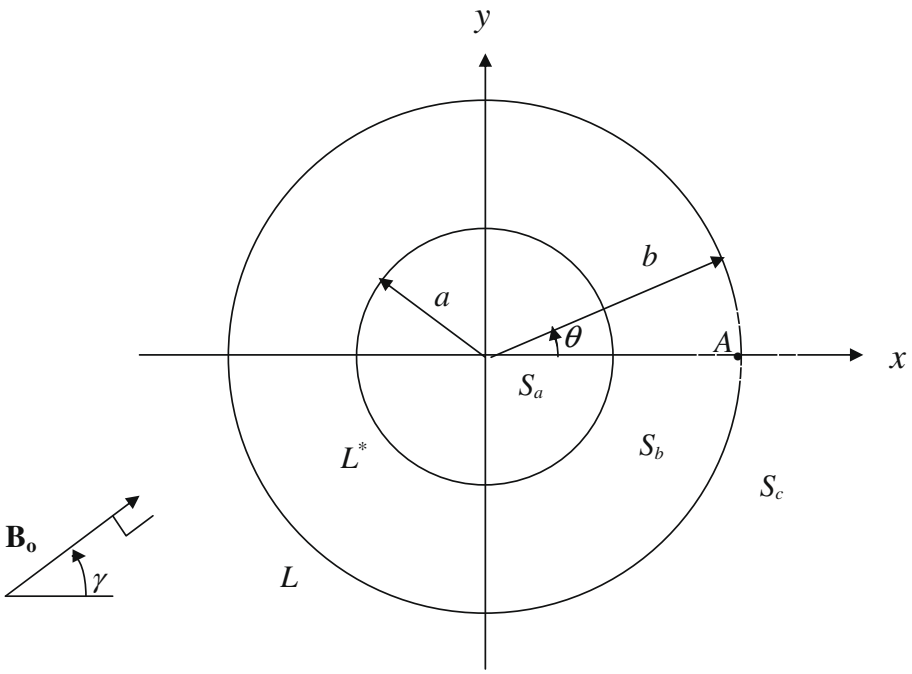

Fig. 1. A three-phase cylinder subjected to a remote uniform magnetic induction.

where $\rho_b = be^{i\theta}$ with the phase angle θ shown in Fig. 1. Via the use of analytic continuation, we have

$$h_1(z) = h_0(z) + \bar{h}_{c0}\left(\frac{b^2}{z}\right) \quad z \in S_a \cup S_b \tag{7}$$

$$\mu_{rb} h_1(z) = \mu_{rc}\left[h_0(z) - \bar{h}_{c0}\left(\frac{b^2}{z}\right)\right] \quad z \in S_a \cup S_b \tag{8}$$

which is holomorphic in the interior region $S_a \cup S_b$ and

$$\bar{h}_1\left(\frac{b^2}{z}\right) = \bar{h}_0\left(\frac{b^2}{z}\right) + h_{c0}(z) \quad z \in S_c \tag{9}$$

$$\mu_{rb}\bar{h}_1\left(\frac{b^2}{z}\right) = \mu_{rc}\left[\bar{h}_0\left(\frac{b^2}{z}\right) - h_{c0}(z)\right] \quad z \in S_c \tag{10}$$

is holomorphic in the exterior region S_c. It is remarked that the symbol $\bar{h}_{c0}(b^2/z)$ indicates that the complex conjugate of the coefficients (rather than argument) in the corresponding function is taken. The complex potential functions $h_1(z)$ and $h_{c0}(z)$ can be solved from Eqs. (7)–(10) as

$$h_1(z) = U_{bc} h_0(z), \quad h_{c0}(z) = V_{bc}\bar{h}_0\left(\frac{b^2}{z}\right) \tag{11}$$

where

$$U_{bc} = \frac{2\mu_{rc}}{\mu_{rc} + \mu_{rb}}, \quad V_{bc} = \frac{\mu_{rc} - \mu_{rb}}{\mu_{rc} + \mu_{rb}} \tag{12}$$

Step 2: analytic continuation across the interface L^*

In this step, it is assumed that the region S_a is made of material a and the regions S_b and S_c are composed of the same material b. The complex potential function $h_1(z)$, which is holomorphic in the interior region $S_a \cup S_b$ as shown in Eq. (4), will induce a complex potential function $h_{a1}(z)$ holomorphic in the interior region S_a and a complex potential function $h_{b1}(z)$ holomorphic in the exterior region $S_b \cup S_c$. Thus the boundary conditions of magnetic fields yield

$$h_{a1}(\rho_a) + \overline{h_{a1}(\rho_a)} = h_1(\rho_a) + \overline{h_1(\rho_a)} + h_{b1}(\rho_a) + \overline{h_{b1}(\rho_a)} \tag{13}$$

$$\mu_{ra}\left[h_{a1}(\rho_a) - \overline{h_{a1}(\rho_a)}\right] = \mu_{rb}\left[h_1(\rho_a) - \overline{h_1(\rho_a)} + h_{b1}(\rho_a) - \overline{h_{b1}(\rho_a)}\right] \tag{14}$$

where $\rho_a = ae^{i\theta}$. By the use of analytic continuation, one can obtain

$$h_{a1}(z) = h_1(z) + \bar{h}_{b1}\left(\frac{a^2}{z}\right) \quad z \in S_a \tag{15}$$

$$\mu_{ra} h_{a1}(z) = \mu_{rb}\left[h_1(z) - \bar{h}_{b1}\left(\frac{a^2}{z}\right)\right] \quad z \in S_a \tag{16}$$

and

$$\bar{h}_{a1}\left(\frac{a^2}{z}\right) = \bar{h}_1\left(\frac{a^2}{z}\right) + h_{b1}(z) \quad z \in S_b \cup S_c \tag{17}$$

$$\mu_{ra}\left[\bar{h}_{a1}\left(\frac{a^2}{z}\right)\right] = \mu_{rb}\left[\bar{h}_1\left(\frac{a^2}{z}\right) - h_{b1}(z)\right] \quad z \in S_b \cup S_c \tag{18}$$

The complex potential functions $h_{a1}(z)$ and $h_{b1}(z)$ can be found from Eqs. (15)–(18) as

$$h_{a1}(z) = U_{ab} h_1(z), \quad h_{b1}(z) = V_{ab}\bar{h}_1\left(\frac{a^2}{z}\right) \tag{19}$$

where

$$U_{ab} = \frac{2\mu_{rb}}{\mu_{rb} + \mu_{ra}}, \quad V_{ab} = \frac{\mu_{rb} - \mu_{ra}}{\mu_{rb} + \mu_{ra}} \tag{20}$$

Step 3: analytic continuation across the interface L

Just like that in step 1, the regions S_a and S_b are composed of the same material b and the region S_c is consisted of material c in this step. Thus the complex potential function $h_{b1}(z)$, which is holomorphic in the exterior region $S_b \cup S_c$ as shown in Eq. (17), will cause a complex potential function $h_2(z)$ holomorphic in the interior region $S_a \cup S_b$ and a complex potential function $h_{c1}(z)$ holomorphic in the exterior region S_c. Similar to the solving process given in step 1, one can apply the boundary conditions of magnetic filed across L to obtain

$$h_{b1}(\rho_b) + \overline{h_{b1}(\rho_b)} + h_2(\rho_b) + \overline{h_2(\rho_b)} = h_{c1}(\rho_b) + \overline{h_{c1}(\rho_b)} \tag{21}$$

$$\mu_{rb}\left[h_{b1}(\rho_b) - \overline{h_{b1}(\rho_b)} + h_2(\rho_b) - \overline{h_2(\rho_b)}\right] = \mu_{rc}\left[h_{c1}(\rho_b) - \overline{h_{c1}(\rho_b)}\right] \tag{22}$$

Therefore, these equations can be solved by employing the method of analytic continuation. It renders

$$h_2(z) = V_{cb}\bar{h}_{b1}\left(\frac{b^2}{z}\right), \quad h_{c1}(z) = U_{cb} h_{b1}(z) \tag{23}$$

Step 4: repetition of steps 2 and 3

Applying the method of analytic continuation repeatedly across two interfaces L^* and L just like that in steps 2 and 3, one can find the increments of the complex potential functions $h_{an}(z)$, $h_{bn}(z)$, $h_{cn}(z)$ and $h_{n+1}(z)$ for $n = 2,3,4,\ldots$. The alternating technique denotes such processes. Taking the summation of all the increments will form the complete solution of magnetic potential function as

$$h(z) = \begin{cases} \sum_{n=1}^{\infty} h_{an}(z) & z \in S_a \\ \sum_{n=1}^{\infty} [h_n(z) + h_{bn}(z)] & z \in S_b \\ h_0(z) + \sum_{n=0}^{\infty} h_{cn}(z) & z \in S_c \end{cases} \tag{24}$$

Referring to Eqs. (19) and (23), the functions $h_{an}(z)$, $h_{bn}(z)$ and $h_{cn}(z)$ can be expressed in terms of $h_n(z)$ for $n \geqslant 1$. By the use of such expressions and Eq. (11), the function $h(z)$ becomes

$$h(z) = \begin{cases} U_{ab}\sum_{n=1}^{\infty} h_n(z) & z \in S_a \\ \sum_{n=1}^{\infty}\left[h_n(z) + V_{ab}\bar{h}_n\left(\frac{a^2}{z}\right)\right] & z \in S_b \\ h_0(z) + V_{bc}\bar{h}_0\left(\frac{b^2}{z}\right) + U_{cb}V_{ab}\sum_{n=1}^{\infty}\bar{h}_n\left(\frac{a^2}{z}\right) & z \in S_c \end{cases} \tag{25}$$

The recurrence formula of $h_n(z)$ can be derived from Eqs. (11), (19) and (23). It gives

$$h_{n+1}(z) = \begin{cases} U_{bc} h_0(z) & \text{for } n = 0 \\ V_{cb} V_{ab} h_n\left(\frac{a^2}{b^2} z\right) & \text{for } n = 1, 2, 3, \ldots \end{cases} \tag{26}$$

As mentioned in the previous paragraph, the corresponding complex potential function for a remote uniform magnetic induction can be written as

$$h_0(z) = H_0 e^{-i\gamma} z \tag{27}$$

where

$$H_0 = \frac{B_0}{\mu_0 \mu_{rc}} \tag{28}$$

Referring to Eqs. (12) and (20), the quantities V_{cb} and V_{ab} are found to be less than 1. Thus $\sum_{n=1}^{\infty} h_n(z)$ is a convergent series and the substitution of $h_0(z)$ into Eqs. (25) and (26) gives rise to

$$h(z) = \begin{cases} \frac{U_{ab} U_{bc} H_0 e^{-i\gamma}}{1 - \frac{a^2}{b^2} V_{cb} V_{ab}} z & z \in S_a \\ \frac{U_{bc} H_0}{1 - \frac{a^2}{b^2} V_{cb} V_{ab}} \left(e^{-i\gamma} z + V_{ab} e^{i\gamma} \frac{a^2}{z} \right) & z \in S_b \\ H_0 \left[e^{-i\gamma} z + \left(V_{bc} \frac{b^2}{a^2} + \frac{U_{cb} V_{ab} U_{bc}}{1 - \frac{a^2}{b^2} V_{cb} V_{ab}} \right) \frac{a^2 e^{i\gamma}}{z} \right] & z \in S_c \end{cases} \tag{29}$$

3. Magnetoelastic field

The components of traction force and displacement can be represented in terms of two complex potential functions $\phi(z)$ and $\psi(z)$ of magnetoelastic stress fields as [13]

$$f_x + i f_y = -i \left[\phi(z) + z\overline{\phi'(z)} + \overline{\psi(z)} + \frac{G\mu_0\chi}{(\lambda + 2G)} h(z)\overline{h'(z)} - \frac{\mu_0(\mu_r + \chi)}{2} \int_A^B \overline{h'(z) h'(z)} d\bar{z} \right] \tag{30}$$

$$u_x + i u_y = \frac{1}{2G} \left[\kappa\phi(z) - z\overline{\phi'(z)} - \overline{\psi(z)} - \frac{G\mu_0\chi}{(\lambda + 2G)} h(z)\overline{h'(z)} \right] \tag{31}$$

where G is the shear modulus, $\kappa = (\lambda + 3G)/(\lambda + G) = 3 - 4\nu$ for plane strain with ν being the Poisson's ratio [14] and $\chi (= \mu_r - 1)$ denotes the magnetic susceptibility. It is remarked that Eqs. (30) and (31) are continuous across the material boundary and those terms related to body force are omitted in these two equations. The magnetoelastic stresses in polar coordinates can be expressed with $\phi(z)$ and $\psi(z)$ as [15]

$$t_{rr} + t_{\theta\theta} = 2\left[\phi'(z) + \overline{\phi'(z)} \right] - \frac{\lambda\mu_0\chi}{\lambda + 2G} h'(z)\overline{h'(z)} \tag{32}$$

$$\begin{aligned} (t_{rr} + i t_{r\theta}) = {} & \left[\phi'(z) + \overline{\phi'(z)} \right] - \frac{\lambda\mu_0\chi}{2(\lambda + 2G)} h'(z)\overline{h'(z)} \\ & - \left\{ z\overline{\phi''(z)} + \overline{\psi'(z)} + \frac{G\mu_0\chi}{\lambda + 2G} h(z)\overline{h''(z)} - \frac{\mu_0\chi}{2} \overline{h'(z) h'(z)} \right\} \frac{\bar{z}}{z} \end{aligned} \tag{33}$$

Since there are circular interfaces in the present problem, it is convenient to rearranged Eqs. (30) and (31) for a region bounded by a circle $r = c$ as

$$\begin{aligned} -f_y + i f_x = {} & \phi(z) + \overline{\omega(z)} - \left(\frac{c^2}{\bar{z}} - z \right) \overline{\phi'(z)} + \frac{G\mu_0\chi}{(\lambda + 2G)} h(z) \left[\overline{h'(z)} - \overline{h'}\left(\frac{c^2}{z} \right) \right] \\ & + \frac{G\mu_0\chi}{(\lambda + 2G)} h(z)\overline{h'}\left(\frac{c^2}{z} \right) - \frac{\mu_0(\mu_r + \chi)}{2} \overline{\eta(z)} \end{aligned} \tag{34}$$

$$u_x + i u_y = \frac{1}{2G} \left\{ \kappa\phi(z) - \overline{\omega(z)} + \left(\frac{c^2}{\bar{z}} - z \right) \overline{\phi'(z)} - \frac{G\mu_0\chi}{(\lambda + 2G)} h(z) \left[\overline{h'(z)} - \overline{h'}\left(\frac{c^2}{z} \right) \right] - \frac{G\mu_0\chi}{(\lambda + 2G)} h(z)\overline{h'}\left(\frac{c^2}{z} \right) \right\} \tag{35}$$

where

$$\omega(z) = \frac{c^2}{z} \phi'(z) + \psi(z), \quad \eta(z) = \int_A^B h'(z) h'(z) dz \tag{36}$$

The corresponding magnetoelastic stresses in Eq. (33) becomes

$$\begin{aligned} t_{rr}+\mathrm{i}t_{r\theta} &= \phi'(z)-\frac{\bar{z}}{z}\overline{\omega'(z)}+\left(1-\frac{c^2}{z\bar{z}}\right)\overline{\phi'(z)}+\left(\frac{c^2}{z}-\bar{z}\right)\overline{\phi''(z)}+\overline{\phi'(z)}-\frac{\lambda\mu_0\chi}{2(\lambda+2G)}h'(z)\overline{h'}\left(\frac{c^2}{z}\right)\\ &\quad-\frac{\lambda\mu_0\chi}{2(\lambda+2G)}h'(z)\left[\overline{h'(z)}-\overline{h'}\left(\frac{c^2}{z}\right)\right]-\frac{G\mu_0\chi}{\lambda+2G}\frac{\bar{z}}{z}h(z)\overline{h''}\left(\frac{c^2}{z}\right)-\frac{G\mu_0\chi}{\lambda+2G}\frac{\bar{z}}{z}h(z)\left[\overline{h''(z)}-\overline{h''}\left(\frac{c^2}{z}\right)\right]\\ &\quad+\frac{\mu_0\chi}{2}\frac{\bar{z}}{z}\overline{h'}\left(\frac{c^2}{z}\right)\overline{h'}\left(\frac{c^2}{z}\right)+\frac{\mu_0\chi}{2}\frac{\bar{z}}{z}\left[\overline{h'(z)h'(z)}-\overline{h'}\left(\frac{c^2}{z}\right)\overline{h'}\left(\frac{c^2}{z}\right)\right] \end{aligned} \tag{37}$$

Notice that both Eqs. (34) and (35) are also continuous across the boundary of material interface. By applying the alternating technique with the magnetic fields in Eq. (25), the magnetoelastic fields on the trimaterial cylinder under a uniform magnetic induction can be found.

Step 1: analytic continuation across the interface L

In the first step, the regions S_a and S_b are regarded to be composed of the same material b and the region S_c is consisted of material c. The magnetoelastic potential functions can be represent as

$$\phi_{1b}(z)=\begin{cases}\phi_{bm}(z)\\ \phi_{cm}(z)\end{cases},\ \omega_{1b}=\begin{cases}\omega_{bm}(z) & z\in S_a\cup S_b\\ \omega_{cm}(z) & z\in S_c\end{cases} \tag{38}$$

where the subscript $1b$ in $h_{1b}(z)$ denotes the first time to consider the continuity conditions across the interface L(i.e. $r=b$). The complex potential functions $\phi_{bm}(z)$ and $\omega_{bm}(z)$ are holomorphic in the interior region $S_a\cup S_b$, $\phi_{cm}(z)$ and $\omega_{cm}(z)$ are holomorphic in the exterior region S_c. Using Eq. (29) and replacing c with b in Eqs. (34) and (35), the continuity conditions of traction and displacement across the material interface L render

$$\begin{aligned} &\phi_{bm}(\rho_b)+\overline{\omega_{bm}(\rho_b)}+\frac{G_b\mu_0\chi_b}{\lambda_b+2G_b}h_b(\rho_b)\overline{h_b'(\rho_b)}-\frac{\mu_0(\mu_{rb}+\chi_b)}{2}\overline{\eta_b(\rho_b)}=\phi_{cm}(\rho_b)+\overline{\omega_{cm}(\rho_b)}\\ &\quad+\frac{G_c\mu_0\chi_c}{\lambda_c+2G_c}h_c(\rho_b)\overline{h_c'(\rho_b)}-\frac{\mu_0(\mu_{rc}+\chi_c)}{2}\overline{\eta_c(\rho_b)} \end{aligned} \tag{39}$$

$$\frac{1}{2G_b}\left[\kappa_b\phi_{bm}(\rho_b)-\overline{\omega_{bm}(\rho_b)}-\frac{G_b\mu_0\chi_b}{\lambda_b+2G_b}h_b(\rho_b)\overline{h_b'(\rho_b)}\right]=\frac{1}{2G_c}\left[\kappa_c\phi_{cm}(\rho_b)-\overline{\omega_{cm}(\rho_b)}-\frac{G_c\mu_0\chi_c}{\lambda_c+2G_c}h_c(\rho_b)\overline{h_c'(\rho_b)}\right] \tag{40}$$

where $\rho_b=be^{\mathrm{i}\theta}$ was defined in the previous section. The complex potential functions

$$\begin{aligned} h_b(z)&=\frac{U_{bc}H_0}{1-\frac{a^2}{b^2}V_{cb}V_{ab}}\left(e^{-\mathrm{i}\gamma}z+V_{ab}e^{\mathrm{i}\gamma}\frac{a^2}{z}\right),\\ h_c(z)&=H_0\left(e^{-\mathrm{i}\gamma}z+V_{bc}e^{\mathrm{i}\gamma}\frac{b^2}{z}+\frac{U_{cb}V_{ab}U_{bc}e^{\mathrm{i}\gamma}}{1-\frac{a^2}{b^2}V_{cb}V_{ab}}\frac{a^2}{z}\right) \end{aligned} \tag{41}$$

are the expression of $h(z)$ in Eq. (29) within the regions S_b and S_c, respectively. In Eqs. (39) and (40), the function $\eta(z)$ can be expressed with the corresponding function $h(z)$ as

$$\eta_s(z)=\int_A^B h_s'(z)h_s'(z)dz\ s=a,b,c \tag{42}$$

Before separating (39) and (40) into two parts which are holomorphic in both interior region $S_a\cup S_b$ and exterior region S_c, respectively, the estimation

$$\lim_{z\to\infty}\overline{\omega_{bm}}\left(\frac{b^2}{z}\right)=\lim_{z\to\infty}\left[z\overline{\phi_{bm}'}\left(\frac{b^2}{z}\right)+\overline{\psi_{bm}}\left(\frac{b^2}{z}\right)\right]\approx z\overline{\phi_{bm}'}(0)+\overline{\psi_{bm}}(0) \tag{43}$$

can be derived from Eq. (36) by replacing c with b. Such an estimation guarantees that $\overline{\omega_{bm}}(b^2/z)-z\overline{\phi'}_{bm}(0)$ is holomorphic in the exterior region S_c. Furthermore, when the applied magnetic induction impinges into the region S_c, the limiting values of magnetoelastic complex potential functions $\phi_{cm}'(z)$ and $\psi_{cm}'(z)$ at infinity satisfy [11]

$$\begin{aligned} \phi_{cm}'(z)&=\Gamma+\frac{B_0^2}{2\mu_0}\left(\frac{1}{4}-\frac{\chi_c}{\mu_{rc}^2}\right)+O\left(\frac{1}{z}\right),\\ \psi_{cm}'(z)&=\Gamma'-\frac{B_0^2e^{-2\mathrm{i}\gamma}}{2\mu_0}\left(\frac{1}{2}-\frac{\mu_{rc}+\chi_c}{\mu_{rc}^2}\right)+O\left(\frac{1}{z}\right)\quad\text{for } |z|\gg 1 \end{aligned} \tag{44}$$

where

$$\Gamma=\frac{1}{4}(\sigma_1^\infty+\sigma_2^\infty)+\mathrm{i}\frac{2G\omega^\infty}{1+\kappa},\quad \Gamma'=-\frac{1}{2}(\sigma_1^\infty-\sigma_2^\infty)e^{-2\mathrm{i}\varpi} \tag{45}$$

in which the symbols σ_1^∞ and σ_2^∞ are the applied principal mechanical stresses along x_1 and x_2 directions at infinity and the symbol

$$\omega^\infty = \mathrm{Im}(\partial D/\partial z) \tag{46}$$

denotes the rotation at infinity. Since the effect of magnetic loading is dominant in this study, those terms, which is related to pure mechanical loading, is discarded in the following paragraph, i.e. $\Gamma = \Gamma' = 0$.

Via the use of analytic continuation across the interface L, the potential functions $\phi_{bm}(z)$, $\omega_{bm}(z)$, $\phi_{cm}(z)$ and $\omega_{bm}(z)$ can be solved as shown in the Appendix A. It is noted that the Dundurs parameters [16]

$$\Lambda_{ab} = \frac{\alpha_{ab} + \beta_{ab}}{1 - \beta_{ab}}, \quad \Pi_{ab} = \frac{\alpha_{ab} - \beta_{ab}}{1 + \beta_{ab}} \tag{47}$$

with

$$\alpha_{ab} = \frac{G_a(\kappa_b + 1) - G_b(\kappa_a + 1)}{G_a(\kappa_b + 1) + G_b(\kappa_a + 1)}, \quad \beta_{ab} = \frac{G_a(\kappa_b - 1) - G_b(\kappa_a - 1)}{G_a(\kappa_b + 1) + G_b(\kappa_a + 1)} \tag{48}$$

are introduced in this solving process.

Step 2: analytic continuation across the interface L^*

In this step, it is assumed that the region S_a is made of material a and the regions S_b and S_c are composed of the same material b. The complex potential functions $\phi_{bm}(z)$ and $\omega_{bm}(z)$, which are holomorphic in the interior region $S_a \cup S_b$ as shown in Eqs. (A6) and (A7), will induce two complex potential functions $\phi_{am}(z)$ and $\omega_{am}(z)$ in the interior region S_a and two complex potential function $\phi_{b0}(z)$ and $\omega_{b0}(z)$ in the exterior region $S_b \cup S_c$. Using Eq. (29) and replacing c with a in Eqs. (34) and (35), the continuity conditions of traction and displacement across the material interface L^* give rise to

$$\begin{aligned}
&\phi_{am}(\rho_a) + \overline{\omega_{am}(\rho_a)} + \frac{G_a\mu_0\chi_a}{\lambda_a + 2G_a} h_a(\rho_a)\overline{h_a'(\rho_a)} - \frac{\mu_0(\mu_{ra} + \chi_a)}{2}\overline{\eta_a(\rho_a)} \\
&\quad = \phi_{bm}(\rho_a) + \phi_{b0}(\rho_a) + \overline{\omega_{bm}^a(\rho_a)} + \overline{\omega_{b0}(\rho_a)} + \frac{G_b\mu_0\chi_b}{\lambda_b + 2G_b} h_b(\rho_a)\overline{h_b'(\rho_a)} - \frac{\mu_0(\mu_{rb} + \chi_b)}{2}\overline{\eta_b(\rho_a)}
\end{aligned} \tag{49}$$

$$\begin{aligned}
&\frac{1}{2G_a}\left[\kappa_a\phi_{am}(\rho_a) - \overline{\omega_{am}(\rho_a)} - \frac{G_a\mu_0\chi_a}{\lambda_a + 2G_a} h_a(\rho_a)\overline{h_a'(\rho_a)}\right] \\
&\quad = \frac{1}{2G_b}\left[\kappa_b\phi_{bm}(\rho_a) + \kappa_b\phi_{b0}(\rho_a) - \overline{\omega_{bm}^a(\rho_b)} - \overline{\omega_{b0}(\rho_a)} - \frac{G_b\mu_0\chi_b}{\lambda_b + 2G_b} h_b(\rho_a)\overline{h_b'(\rho_a)}\right]
\end{aligned} \tag{50}$$

where $\rho_a = ae^{i\theta}$ and the function $\eta_a(z)$ is defined in Eq. (42). From the definition of $\omega(z)$ in Eq. (36), we have

$$\omega_{bm}(z) = \frac{b^2}{z}\phi_{bm}'(z) + \psi_{bm}(z) = \frac{a^2}{z}\phi_{bm}'(z) + \psi_{bm}(z) + \frac{b^2 - a^2}{z}\phi_{bm}'(z) = \omega_{bm}^a(z) + \frac{b^2 - a^2}{z}\phi_{bm}'(z) \tag{51}$$

and hence

$$\omega_{bm}^a(z) = \omega_{bm}(z) + \frac{a^2 - b^2}{z}\phi_{bm}'(z) \tag{52}$$

which denotes the function with the circular boundary $r = a$ corresponding to $\omega_{bm}(z)$ with the circular boundary $r = b$.

By the use of analytic continuation across the interface L^*, the potential functions $\phi_{bm}(z)$, $\omega_{bm}(z)$, $\phi_{cm}(z)$ and $\omega_{bm}(z)$ are derived in the Appendix B. It is noted that the complex potential function $\phi_{b0}(z)$ and $\omega_{b0}(z)$ have the form

$$\phi_{b0}(z) = K\frac{a^2}{z}, \quad \omega_{b0}(z) = N_1\frac{a^2}{z} + N_3\frac{a^4}{z^3} \quad z \in S_b \cup S_c \tag{53}$$

where

$$\begin{aligned}
K = \mu_0 H_0^2 \Bigg\{ &\frac{\Pi_{ab}\chi_b G_b}{\lambda_b + 2G_b}\frac{H^2}{H_0^2}\left[\frac{\Pi_{cb}}{1 - \Pi_{cb}}\left(1 - V_{ab}^2\frac{a^4}{b^4} - 3V_{ab}e^{2i\gamma}\frac{a^2}{b^2}\frac{a^2 - b^2}{b^2}\right) + V_{ab}e^{2i\gamma}\frac{b^2 - a^2}{b^2}\right] \\
&+ \Pi_{ab}G_b(\mu_{rb} + \chi_b)\frac{H^2}{H_0^2}\left[\frac{V_{ab}}{G_b + \kappa_b G_c}\frac{a^2}{b^2} + \frac{\kappa_c e^{2i\gamma}}{2(G_c + \kappa_c G_b)} - \frac{V_{ab}^2 e^{2i\gamma}}{2(1 - \Pi_{cb})(G_b + \kappa_b G_c)}\frac{a^4(a^2 - b^2)}{b^6} + \frac{e^{2i\gamma}}{2\Pi_{ab}(G_b + \kappa_b G_a)}\right] \\
&+ \Pi_{ab}(1 + \Pi_{bc})\mu_{rc}^2\overline{W}e^{2i\gamma} - \Pi_{ab}G_b(\mu_{rc} + \chi_c)\left[\frac{\kappa_c e^{2i\gamma}}{2(G_c + \kappa_c G_b)} + \frac{1}{(G_b + \kappa_b G_c)}\left(V_{bc} + U_{cb}V_{ab}\frac{H}{H_0}\frac{a^2}{b^2}\right)\right. \\
&\left. - \frac{e^{-2i\gamma}}{2(1 - \Pi_{cb})(G_b + \kappa_b G_c)}\left(V_{bc} + U_{cb}V_{ab}\frac{H}{H_0}\frac{a^2}{b^2}\right)^2\frac{a^2 - b^2}{b^2}\right] + \frac{\Pi_{ab}(1 + \Pi_{bc})\chi_c G_c}{\lambda_c + 2G_c}\left(V_{bc} + U_{cb}V_{ab}\frac{H}{H_0}\frac{a^2}{b^2}\right) - \frac{(\mu_{ra} + \chi_a)U_{ab}^2 G_b e^{2i\gamma}}{2(G_b + \kappa_b G_a)}\frac{H^2}{H_0^2}\Bigg\}
\end{aligned} \tag{54}$$

and

$$N_1 = \mu_0 H_0^2 \Bigg\{ \Bigg[\frac{\chi_a G_a U_{ab}^2}{\lambda_a + 2G_a} \left(1 + \Pi_{ba} + \frac{\Pi_{ba}}{1-\Pi_{ba}} \frac{G_b}{G_a + \kappa_a G_b} \right) - \frac{\chi_b G_b}{\lambda_b + 2G_b} (1 - V_{ab}^2) + (\mu_{rb} + \chi_b) V_{ab} \left(\frac{\kappa_a G_b}{G_a + \kappa_a G_b} - \frac{1}{1-\Pi_{ba}} \frac{G_a}{G_a + \kappa_a G_b} + \frac{1}{1-\Pi_{cb}} \frac{G_b}{G_b + \kappa_b G_c} \frac{a^2}{b^2} \right) \Bigg] \frac{H^2}{H_0^2} + \Lambda_{ab}(1 + \Lambda_{bc}) \mu_{rc}^2 \overline{T} + \frac{1}{1-\Pi_{cb}} \Bigg[\frac{\chi_b G_b \Pi_{cb}}{\lambda_b + 2G_b} \frac{H}{H_0} \left(1 - V_{ab}^2 \frac{a^4}{b^4} \right) - \frac{G_b(\mu_{rc} + \chi_c)}{G_b + \kappa_b G_c} \left(V_{bc} + U_{cb} V_{ab} \frac{H}{H_0} \frac{a^2}{b^2} \right) \left(\Lambda_{ab} - \frac{a^2 - b^2}{a^2} + \frac{1 + \Lambda_{ab}}{1 - \Pi_{ba}} \frac{G_b}{G_a + \kappa_a G_b} \right) \Bigg] \Bigg\} \tag{55}$$

$$N_3 = \mu_0 H_0^2 \Bigg\{ \Bigg[\left(\frac{\chi_b}{\lambda_b + 2G_b} - \frac{\Lambda_{ab} \Pi_{cb} \chi_b}{\lambda_b + 2G_b} \frac{a^4}{b^4} \right) - \frac{\mu_{rb} + \chi_b}{6} \left(\frac{\kappa_a}{G_a + \kappa_a G_b} + \frac{\Lambda_{ab}}{G_b + \kappa_b G_c} \frac{a^6}{b^6} \right) V_{ab} \Bigg] \frac{H^2}{H_0^2} G_b V_{ab} e^{2i\gamma} + \frac{\Lambda_{ab} G_b (\mu_{rc} + \chi_c) e^{-2i\gamma}}{6(G_b + \kappa_b G_c)} \left(V_{bc} + U_{cb} V_{ab} \frac{H}{H_0} \frac{a^2}{b^2} \right)^2 \frac{a^2}{b^2} \Bigg\} \tag{56}$$

Step 3: analytic continuation across the interface L

Just like that applied in step 1, the regions S_a and S_b are regarded as the same material b and the region S_c is made of material c. Therefore, both complex potential functions $\phi_{b0}(z)$ and $\omega_{b0}(z)$, which are holomorphic in the exterior region $S_b \cup S_c$ as presented in Eq. (53), will cause two complex potential functions $\phi_1(z)$ and $\omega_1(z)$ in the interior region $S_a \cup S_b$ and two complex potential functions $\phi_{c0}(z)$ and $\omega_{c0}(z)$ in the exterior region S_c. Thus one can employ the continuity conditions of magnetoelastic fields across the interface L to find

$$\phi_{b0}(\rho_b) + \overline{\omega_{b0}^b(\rho_b)} + \phi_1(\rho_b) + \overline{\omega_1(\rho_b)} = \phi_{c0}(\rho_b) + \overline{\omega_{c0}(\rho_b)} \tag{57}$$

$$\frac{1}{2G_b} \left[\kappa_b \phi_{b0}(\rho_b) - \overline{\omega_{b0}^b(\rho_b)} + \kappa_b \phi_1(\rho_b) - \overline{\omega_1(\rho_b)} \right] = \frac{1}{2G_c} \left[\kappa_c \phi_{c0}(\rho_b) - \overline{\omega_{c0}(\rho_b)} \right] \tag{58}$$

where

$$\omega_{b0}^b(z) = \omega_{b0}(z) + \frac{b^2 - a^2}{z} \phi_0'(z) \tag{59}$$

is the function with circular boundary $r = b$ corresponding to $\omega_{b0}(z)$ on the circular boundary of $r = a$. Such a relation is similar to that given in Eq. (52). The application of the analytic continuation on Eqs. (57) and (58) renders

$$\phi_1(z) + \overline{\omega_{b0}^b}\left(\frac{b^2}{z}\right) - \overline{\omega_{c0}}\left(\frac{b^2}{z}\right) + C_1 z = 0 \quad z \in S_a \cup S_b \tag{60}$$

$$\phi_{c0}(z) - \phi_{b0}(z) - \overline{\omega_1}\left(\frac{b^2}{z}\right) + C_1 z = 0 \quad z \in S_c \tag{61}$$

$$\frac{\kappa_b \phi_1(z) - \overline{\omega_{b0}^b}\left(\frac{b^2}{z}\right)}{2G_b} + \frac{\overline{\omega_{c0}}\left(\frac{b^2}{z}\right)}{2G_c} - \frac{C_1 z}{2G_b} = 0 \quad z \in S_a \cup S_b \tag{62}$$

$$\frac{\kappa_c \phi_{c0}(z)}{2G_c} - \frac{\kappa_b \phi_{b0}(z) - \overline{\omega_1}\left(\frac{b^2}{z}\right)}{2G_b} - \frac{C_1 z}{2G_b} = 0 \quad z \in S_c \tag{63}$$

where

$$C_1 = \overline{\phi_1'}(0) \tag{64}$$

Via the use of Eqs. (60)–(63), the complex potential functions $\phi_1(z)$, $\omega_1(z)$, $\phi_{c0}(z)$ and $\omega_{c0}(z)$ can be expressed with $\phi_0(z)$ and $\omega_0(z)$ as

$$\phi_1(z) = \Pi_{cb} \left[\overline{\omega_{b0}}\left(\frac{b^2}{z}\right) + \frac{b^2 - a^2}{b^2} z \overline{\phi_{b0}'}\left(\frac{b^2}{z}\right) + C_1 z \right] \quad z \in S_a \cup S_b \tag{65}$$

$$\omega_1(z) = \Lambda_{cb} \overline{\phi_{b0}}\left(\frac{b^2}{z}\right) + \overline{C_1} \frac{b^2}{z} \quad z \in S_a \cup S_b \tag{66}$$

$$\phi_{c0}(z) = (1 + \Lambda_{cb}) \phi_{b0}(z) \quad z \in S_c \tag{67}$$

$$\omega_{c0}(z) = (1 + \Pi_{cb}) \left[\omega_{b0}(z) + \frac{b^2 - a^2}{z} \phi_{b0}'(z) + \overline{C_1} \frac{b^2}{z} \right] \quad z \in S_c \tag{68}$$

and

$$C_1 = \frac{\Pi_{cb}}{1-\Pi_{cb}^2}\frac{a^2}{b^2}(N_1 + \Pi_{cb}\overline{N_1}) = \frac{\Pi_{cb}}{1-\Pi_{cb}}\frac{a^2}{b^2}N_1 \tag{69}$$

which can be found by substituting Eqs. (53) into (65) and using Eq. (64). The fact that N_1 is real can be observed from Eq. (55) and be applied in the derivation of Eq. (69).

Step 4: analytic continuation across the interface L^*

Similar to that assumed in step 2, the region S_a is composed of material a and the regions S_b and S_c are consisted of the same material b. Thus the complex potential functions $\phi_1(z)$ and $\omega_1(z)$ in Eqs. (65) and (66) within the interior region $S_a \cup S_b$ will induce two complex potential functions $\phi_{a1}(z)$ and $\omega_{a1}(z)$ in the interior region S_a and two complex potential functions $\phi_{b1}(z)$ and $\omega_{b1}(z)$ in the exterior region $S_b \cup S_c$. Thus the continuity conditions of traction and displacement across the interface L^* yield

$$\phi_{a1}(\rho_a) + \overline{\omega_{a1}(\rho_a)} = \phi_1(\rho_a) + \overline{\omega_1^a(\rho_a)} + \phi_{b1}(\rho_a) + \overline{\omega_{b1}(\rho_a)} \tag{70}$$

$$\frac{1}{2G_a}\left[\kappa_a\phi_{a1}(\rho_a) - \overline{\omega_{a1}(\rho_a)}\right] = \frac{1}{2G_b}\left[\kappa_b\phi_1(\rho_a) - \overline{\omega_1^a(\rho_a)} + \kappa_b\phi_{b1}(\rho_a) - \overline{\omega_{b1}(\rho_a)}\right] \tag{71}$$

where

$$\omega_1^a(z) = \omega_1(z) + \frac{a^2-b^2}{z}\phi_1'(z) \tag{72}$$

The meaning of superscript a in $\omega_1^a(z)$ is identical to that adopted in Eq. (52).

$$\phi_{a1}(z) - \phi_1(z) - \overline{\omega_{b1}}\left(\frac{a^2}{z}\right) + C_{a1}z - C_1 z = 0 \quad z \in S_a \tag{73}$$

$$\phi_{b1}(z) + \overline{\omega_1^a}\left(\frac{a^2}{z}\right) - \overline{\omega_{a1}}\left(\frac{a^2}{z}\right) + C_{a1}z - C_1 z = 0 \quad z \in S_b \cup S_c \tag{74}$$

$$\frac{\kappa_a\phi_{a1}(z)}{2G_a} - \frac{\kappa_b\phi_1(z) - \overline{\omega_{b1}}\left(\frac{a^2}{z}\right)}{2G_b} - \frac{C_{a1}z}{2G_a} + \frac{C_1 z}{2G_b} = 0 \quad z \in S_a \tag{75}$$

$$\frac{\kappa_b\phi_{b1}(z) - \overline{\omega_1^a}\left(\frac{a^2}{z}\right)}{2G_b} + \frac{\overline{\omega_{a1}}\left(\frac{a^2}{z}\right)}{2G_a} - \frac{C_{a1}z}{2G_a} + \frac{C_1 z}{2G_b} = 0 \quad z \in S_b \cup S_c \tag{76}$$

where

$$C_{a1} = \overline{\phi_{a1}'}(0) \tag{77}$$

As referring to the estimation in Eq. (43), the appearance of C_1 and C_{a1} in Eqs. (73)–(76) can assure that the terms $\overline{\omega_1^a}(a^2/z) - C_1 z$ and $\overline{\omega_{a1}}(a^2/z) - C_{a1}z$ are holomorphic in the exterior region $S_b \cup S_c$.

By the use of Eqs. (73)–(76), the complex potential functions $\phi_{a1}(z)$, $\omega_{a1}(z)$, $\phi_{b1}(z)$ and $\omega_{b1}(z)$ can be expressed with $\phi_1(z)$ and $\omega_1(z)$ as

$$\phi_{a1}(z) = (1+\Lambda_{ab})\phi_1(z) + \Pi_{ba}C_{a1}z \quad z \in S_a \tag{78}$$

$$\omega_{a1}(z) = (1+\Pi_{ab})\left[\omega_1(z) + \frac{a^2-b^2}{z}\phi_1'(z) - \overline{C_1}\frac{a^2}{z}\right] + \overline{C_{a1}}\frac{a^2}{z} \quad z \in S_a \tag{79}$$

$$\phi_{b1}(z) = \Pi_{ab}\left[\overline{\omega_1}\left(\frac{a^2}{z}\right) + \frac{a^2-b^2}{a^2}z\overline{\phi'}_1\left(\frac{a^2}{z}\right) - C_1 z\right] \quad z \in S_b \cup S_c \tag{80}$$

$$\omega_{b1}(z) = \Lambda_{ab}\overline{\phi_1}\left(\frac{a^2}{z}\right) + (1+\Pi_{ba})\overline{C_{a1}}\frac{a^2}{z} - \overline{C_1}\frac{a^2}{z} \quad z \in S_b \cup S_c \tag{81}$$

and

$$C_{a1} = \frac{1+\Lambda_{ab}}{1-\Pi_{ba}}C_1 = \frac{1+\Lambda_{ab}}{1-\Pi_{ba}}\frac{\Pi_{cb}}{1-\Pi_{cb}}\frac{a^2}{b^2}N_1 \tag{82}$$

Based upon the alternating technique, one can apply the analytic continuation across two interfaces L and L^* repeatedly just like that in steps 3 and 4 to find the additional terms $\phi_{c1}(z)$, $\omega_{c1}(z)$ and $\phi_n(z)$, $\omega_n(z)$, $\phi_{an}(z)$, $\omega_{an}(z)$, $\phi_{bn}(z)$, $\omega_{bn}(z)$, $\phi_{cn}(z)$, $\omega_{cn}(z)(n = 2,3,4,\ldots)$. Thus the magnetoelastic potential functions $\phi(z)$ and $\omega(z)$ can be represented as

$$\phi(z)=\begin{cases}\phi_{am}(z)+\sum_{n=1}^{\infty}\phi_{an}(z) & z\in S_a\\ \phi_{bm}(z)+\sum_{n=1}^{\infty}\phi_{n}(z)+\sum_{n=0}^{\infty}\phi_{bn}(z) & z\in S_b\\ \phi_{cm}(z)+\sum_{n=0}^{\infty}\phi_{cn}(z) & z\in S_c\end{cases} \tag{83}$$

$$\omega(z)=\begin{cases}\omega_{am}(z)+\sum_{n=1}^{\infty}\omega_{an}(z) & z\in S_a\\ \omega_{bm}(z)+\sum_{n=1}^{\infty}\omega_{n}(z)+\sum_{n=0}^{\infty}\omega_{bn}(z) & z\in S_b\\ \omega_{cm}(z)+\sum_{n=0}^{\infty}\omega_{cn}(z) & z\in S_c\end{cases} \tag{84}$$

Similar to that given in Eqs. (65) and (66), the complex potential functions $\phi_{n+1}(z)$ and $\omega_{n+1}(z)$ satisfy

$$\phi_{n+1}(z)=\Pi_{cb}\left[\overline{\omega_{bn}}\left(\frac{b^2}{z}\right)+\frac{b^2-a^2}{b^2}z\overline{\phi'_{bn}}\left(\frac{b^2}{z}\right)+C_{n+1}z\right]\quad z\in S_a\cup S_b \tag{85}$$

$$\omega_{n+1}(z)=\Lambda_{cb}\overline{\phi_{bn}}\left(\frac{b^2}{z}\right)+\overline{C_{n+1}}\frac{b^2}{z}\quad z\in S_a\cup S_b \tag{86}$$

for $n\geqslant 1$. The corresponding potential functions $\phi_{bn}(z)$ and $\omega_{bn}(z)$ can be found as

$$\phi_{bn}(z)=\Pi_{ab}\left[\overline{\omega_{n}}\left(\frac{a^2}{z}\right)+\frac{a^2-b^2}{a^2}z\overline{\phi'_{n}}\left(\frac{a^2}{z}\right)-C_nz\right]\quad z\in S_b\cup S_c \tag{87}$$

$$\omega_{bn}(z)=\Lambda_{ab}\overline{\phi_{n}}\left(\frac{a^2}{z}\right)+\left[(1+\Pi_{ba})\overline{C_{an}}-\overline{C_n}\right]\frac{a^2}{z}\quad z\in S_b\cup S_c \tag{88}$$

which is like that presented in Eqs. (80) and (81). The substitution of Eqs. (86) and (88) into (85) and (87) yields the recurrence formula of $\phi_{n+1}(z)$ and $\phi_{bn}(z)$ for $n\geqslant 1$ as

$$\phi_{n+1}(z)=\Pi_{cb}\left\{\Lambda_{ab}\phi_n\left(\frac{a^2}{b^2}z\right)+[(1+\Pi_{ba})C_{an}-C_n]\frac{a^2}{b^2}z+\frac{b^2-a^2}{b^2}z\overline{\phi'_{bn}}\left(\frac{b^2}{z}\right)+C_{n+1}z\right\} \tag{89}$$

$$\phi_{bn}(z)=\Pi_{ab}\left[\Lambda_{cb}\phi_{b(n-1)}\left(\frac{b^2}{a^2}z\right)+C_n\left(\frac{b^2}{a^2}-1\right)z+\frac{a^2-b^2}{a^2}z\overline{\phi'_{n}}\left(\frac{a^2}{z}\right)\right] \tag{90}$$

The comparison between Eqs. (85)–(88) and Eqs. (65), (66), (80) and (81) reveals that two groups of equations possess the similar form. This means that one can obtain one group of equations from the other group. For example, the replacement of the subscripts 0 and 1 in Eqs. (65) and (66) with n and $n+1$, respectively yields Eqs. (85) and (86). Therefore, the expression with subscript 1 can be extended to that with n. The result that C_n is real and the relation $C_{an}=(1+\Lambda_{ab})C_n/(1-\Pi_{ba})$ can be obtained as referring to Eqs. (69) and (82). Applying such results and substituting Eqs. (53) and (64) into (65), the functions $\phi_{n+1}(z)$ and $\phi_{bn}(z)$ in Eqs. (89) and (90) take the form

$$\phi_{n+1}(z)=C_{n+1}z+E_{n+1}z^3,\quad \phi_{bn}(z)=\frac{S_n}{z}\quad \text{for } n\geqslant 0 \tag{91}$$

The corresponding recurrence formula of the coefficients C_{n+1}, E_{n+1} and S_n can be obtained as

$$C_{n+1}=\frac{2\Pi_{cb}(\Lambda_{ab}+\Pi_{ba})}{(1-\Pi_{cb})(1-\Pi_{ba})}\frac{a^2}{b^2}C_n,\quad E_{n+1}=\Pi_{cb}\left(\Lambda_{ab}\frac{a^6}{b^6}E_n-\frac{b^2-a^2}{b^6}\overline{S_n}\right),$$
$$S_n=\Pi_{ab}\left[\Lambda_{cb}\frac{a^2}{b^2}S_{n-1}+3(a^2-b^2)a^2\overline{E_n}\right]\quad \text{for } n\geqslant 1 \tag{92}$$

It is convenience to introduce the following definitions

$$R=\sum_{n=0}^{\infty}C_{n+1},\quad P=\sum_{n=0}^{\infty}E_{n+1},\quad Q=\sum_{n=0}^{\infty}S_n \tag{93}$$

Hence taking $\sum_{n=1}^{\infty}$ for Eq. (92) and using Eq. (69) give rise to

$$R=\sum_{n=0}^{\infty}C_{n+1}=\frac{\frac{\Pi_{cb}}{1-\Pi_{cb}}\frac{a^2}{b^2}N_1}{1-\frac{2\Pi_{cb}(\Lambda_{ab}+\Pi_{ba})}{(1-\Pi_{cb})(1-\Pi_{ba})}\frac{a^2}{b^2}} \tag{94}$$

$$P-E_1=\Pi_{cb}\left[\Lambda_{ab}\frac{a^6}{b^6}P-\frac{b^2-a^2}{b^6}(\overline{Q}-\overline{S_0})\right] \tag{95}$$

$$Q-S_0=\Pi_{ab}\left[\Lambda_{cb}\frac{a^2}{b^2}Q+3(a^2-b^2)a^2\overline{P}\right] \tag{96}$$

where $S_0=Ka^2$ can be obtained from Eqs. (53) and (91) and $E_1=\Pi_{cb}\left[\overline{N_3}a^4/b^6-\overline{K}(b^2-a^2)a^2/b^6\right]$ can be found from Eqs. (53), (65) and (91). In order to provide the convergence condition of (110), it is convenient to use $\kappa_a=\kappa_b=1.8$ (with $v_a=v_b=0.3$) for the typical materials. Via the use of Eqs. (47) and (48) together with $a<b$, one can estimate the ratio in Eq. (92)

$$\begin{aligned}\frac{2\Pi_{cb}(\Lambda_{ab}+\Pi_{ba})}{(1-\Pi_{cb})(1-\Pi_{ba})}\frac{a^2}{b^2}&=\frac{2(G_c-G_b)[(\kappa_b-1)G_a-(\kappa_a-1)G_b]}{[(\kappa_b-1)G_c+2G_b][(\kappa_a-1)G_b+2G_a]}\frac{a^2}{b^2}=\frac{10(G_c-G_b)(G_a-G_b)}{(2G_c+5G_b)(2G_b+5G_a)}\frac{a^2}{b^2}\\&<\frac{10(G_c-G_b)(G_a-G_b)}{10G_cG_a}\frac{a^2}{b^2}<1\end{aligned} \tag{97}$$

which can assure the convergence of the series in Eq. (94). Similarly, the following estimations

$$\begin{aligned}&\Pi_{ab}=\frac{G_a-G_b}{G_a\kappa_b+G_b}<\frac{G_a}{G_a\kappa_b}<1,\\&\Pi_{ab}\Lambda_{cb}\frac{a^2}{b^2}=\frac{G_a-G_b}{G_a\kappa_b+G_b}\frac{G_c\kappa_b-G_b\kappa_c}{G_b\kappa_c+G_c}\frac{a^2}{b^2}<\frac{G_a}{G_a\kappa_b}\frac{G_c\kappa_b}{G_c}\frac{a^2}{b^2}<1\end{aligned} \tag{98}$$

and Π_{cb}, $\Pi_{cb}\Lambda_{ab}a^2/b^2<1$ can be also found from Eq. (47) and (48) with $a<b$. Thus the series P and Q in Eq. (93) are convergent and can be solved from Eqs. (95) and (96) as

$$\begin{aligned}P&=\frac{\left[\left(1-\Pi_{ab}\Lambda_{cb}\frac{a^2}{b^2}\right)\overline{N_3}+\frac{a^2-b^2}{a^2}\overline{K}\right]\Pi_{cb}\frac{a^4}{b^6}}{\left(1-\Pi_{ab}\Lambda_{cb}\frac{a^2}{b^2}\right)\left(1-\Pi_{cb}\Lambda_{ab}\frac{a^6}{b^6}\right)-3\Pi_{ab}\Pi_{cb}\frac{(a^2-b^2)^2a^2}{b^6}},\\Q&=\frac{\left[3\Pi_{ab}\Pi_{cb}\frac{a^6}{b^6}\frac{a^2-b^2}{a^2}N_3+\left(1-\Pi_{cb}\Lambda_{ab}\frac{a^6}{b^6}\right)K\right]a^2}{\left(1-\Pi_{ab}\Lambda_{cb}\frac{a^2}{b^2}\right)\left(1-\Pi_{cb}\Lambda_{ab}\frac{a^6}{b^6}\right)-3\Pi_{ab}\Pi_{cb}\frac{(a^2-b^2)^2a^2}{b^6}}\end{aligned} \tag{99}$$

The summation of the complex potential functions $\phi_n(z)$ and $\phi_{bn}(z)$ can be obtained from Eqs. (91), (93), (94), and (99) as

$$\begin{aligned}\sum_{n=1}^{\infty}\phi_n(z)=\sum_{n=0}^{\infty}(C_{n+1}z+E_{n+1}z^3)=Rz+Pz^3&=\frac{\frac{\Pi_{cb}}{1-\Pi_{cb}}\frac{a^2}{b^2}N_1z}{1-\frac{2\Pi_{cb}(\Lambda_{ab}+\Pi_{ba})}{(1-\Pi_{cb})(1-\Pi_{ba})}\frac{a^2}{b^2}}\\&+\frac{\left[\left(1-\Pi_{ab}\Lambda_{cb}\frac{a^2}{b^2}\right)\overline{N_3}+\frac{a^2-b^2}{a^2}\overline{K}\right]\Pi_{cb}\frac{a^6}{b^6}}{\left(1-\Pi_{ab}\Lambda_{cb}\frac{a^2}{b^2}\right)\left(1-\Pi_{cb}\Lambda_{ab}\frac{a^6}{b^6}\right)-3\Pi_{ab}\Pi_{cb}\frac{(a^2-b^2)^2a^2}{b^6}}\frac{z^3}{a^2}\end{aligned} \tag{100}$$

$$\sum_{n=0}^{\infty}\phi_{bn}(z)=\sum_{n=0}^{\infty}\frac{S_n}{z}=\frac{Q}{z}=\frac{3\Pi_{ab}\Pi_{cb}\frac{a^6}{b^6}\frac{a^2-b^2}{a^2}N_3+\left(1-\Pi_{cb}\Lambda_{ab}\frac{a^6}{b^6}\right)K}{\left(1-\Pi_{ab}\Lambda_{cb}\frac{a^2}{b^2}\right)\left(1-\Pi_{cb}\Lambda_{ab}\frac{a^6}{b^6}\right)-3\Pi_{ab}\Pi_{cb}\frac{(a^2-b^2)^2a^2}{b^6}}\frac{a^2}{z} \tag{101}$$

The solutions for the summation of the corresponding complex potential functions $\sum_{n=1}^{\infty}\omega_n(z)$, $\sum_{n=0}^{\infty}\omega_{bn}(z)$, $\sum_{n=1}^{\infty}\phi_{an}(z)$, $\sum_{n=1}^{\infty}\omega_{an}(z)$, $\sum_{n=1}^{\infty}\phi_{cn}(z)$ and $\sum_{n=1}^{\infty}\omega_{cn}(z)$ are provided in the Appendix C. Putting Eqs. (A5)–(A8), (A14), (A15) and Eqs. (98)–(101) into Eqs. (83) and (84), the solving process in finding the complex potential functions $\phi(z)$ and $\omega(z)$ is completed. Therefore, the magnetoelastic stresses then can be derived from Eqs. (32) and (33).

4. Special cases

4.1. Ferromagnetic thin shell

For the special case that a ferromagnetic cylindrical thin shell subjected to a uniform magnetic induction, the regions S_a and S_c become air and S_b is a ferromagnetic medium with t/a, $t/b\ll 1$. Where $t(=b-a)$ is the thickness of the thin shell. Thus

$\mu_{ra} = \mu_{rc} = 1$ and $\mu_{rb} \gg 1$ can be taken. Substituting such data into Eqs. (12) and (20) yields $U_{ab} = U_{cb} \approx 2$, $V_{ab} = V_{cb} \approx 1$ and $U_{ba} = U_{bc} \approx 2/\mu_{rb} \ll 1$, $V_{ba} = V_{bc} \approx -1$. It is convenient to introduce $R = (a+b)/2 \approx a$, b as the mean radius of the thin shell. The estimation $H/H_0 \approx (2/\mu_{rb})/(1-a^2/b^2) \approx (2/\mu_{rb})/(2Rt/b^2) \approx R/(\mu_{rb}t) \ll 1$ is adopted in the following derivation as that suggested by Lin and Chen [12]. Furthermore, one can find $G_a = G_c = 0$ for the air medium in S_a and S_c and obtain $\Pi_{ab} = \Pi_{cb} = \Lambda_{ab} = \Lambda_{cb} = -1$ via Eqs. (47) and (48). Notice that those terms T and W in Eq. (A5) are induced by the jump of magnetic properties across the interface when the applied magnetic induction comes from the air at infinity to the outer region S_c. Thus both terms disappear for the present case that the outer region S_c is composed of air. Applying the above estimations and $\chi_c = \mu_{rc} - 1 = 0$ on Eqs. (A6), (54)–(56) and discarding those terms with order $1/\mu_{rb}$ and t/R, one can obtain

$$\phi_{bm}(z) \approx \frac{\mu_0 H_0^2 z}{2} - \frac{\mu_0 H_0^2 e^{2i\gamma}}{6}\frac{z^3}{a^2}, \quad K \approx \left(\frac{e^{2i\gamma}}{2} - 1\right)\mu_0 H_0^2, \quad N_1 \approx -\frac{\mu_0 H_0^2}{2}, \quad N_3 \approx \frac{\mu_0 H_0^2 e^{-2i\gamma}}{6} \tag{102}$$

Since the cylindrical shell is axis symmetric, it is convenient to assume that the applied magnetic field propagates along x-axis, i.e. $\gamma = 0$. Substituting Eq. (102) into Eqs. (100) and (101) with the above estimations yields

$$\begin{aligned}
\sum_{n=1}^{\infty}\phi_n(z) &= \frac{-\frac{1}{2}\frac{a^2}{b^2}N_1 z}{1-\frac{a^2}{b^2}} + \frac{\left[\left(1-\frac{a^2}{b^2}\right)\overline{N_3} + \frac{a^2-b^2}{a^2}\overline{K}\right]\Pi_{cb}\frac{a^6}{b^6}}{\left(1-\frac{a^2}{b^2}\right)\left(1-\frac{a^6}{b^6}\right) - 3\frac{(a^2-b^2)^2a^2}{b^6}}\frac{z^3}{a^2} \\
&\approx \frac{\frac{\mu_0 H_0^2}{4}\frac{a^2}{b^2}z}{1-\frac{a^2}{b^2}} + \frac{\left[\left(1-\frac{a^2}{b^2}\right)\frac{\mu_0 H_0^2}{6} - \left(\frac{a^2}{b^2}-1\right)\frac{b^2}{a^2}\frac{\mu_0 H_0^2}{2}\right]\Pi_{cb}\frac{a^6}{b^6}}{\left(1-\frac{a^2}{b^2}\right)^4}\frac{z^3}{a^2} \\
&\approx \mu_0 H_0^2\left(\frac{a^2 z}{8Rt} - \frac{a^4 z^3}{12R^3 t^3}\right), \\
\sum_{n=0}^{\infty}\phi_{bn}(z) &= \frac{3\frac{a^6}{b^6}\frac{a^2-b^2}{a^2}N_3 + \left(1-\frac{a^6}{b^6}\right)K}{\left(1-\frac{a^2}{b^2}\right)\left(1-\frac{a^6}{b^6}\right) - 3\frac{(a^2-b^2)^2a^2}{b^6}}\frac{a^2}{z} \\
&\approx \frac{-3\frac{a^4}{b^4}\left(1-\frac{a^2}{b^2}\right)\frac{\mu_0 H_0^2}{6} - \left(1-\frac{a^2}{b^2}\right)\left(1+\frac{a^2}{b^2}+\frac{a^4}{b^4}\right)\frac{\mu_0 H_0^2}{2}}{\left(1-\frac{a^2}{b^2}\right)^4}\frac{a^2}{z} \approx -\frac{\mu_0 H_0^2 b^6}{4R^3 t^3}\frac{a^2}{z}
\end{aligned} \tag{103}$$

Using Eqs. (29), (83), (102) and (103) with $U_{bc} \approx 2/\mu_{rb} \ll 1$, $H_0 = B_0/\mu_0$, $a = R - t/2$ and $b = R + t/2$, the tangential stress on the outer surface of the cylindrical thin shell can be found as

$$\begin{aligned}
t_{\theta\theta} &\approx \left\{2\left[\phi'(z) + \overline{\phi'(z)}\right] - \frac{\lambda\mu_0\chi}{\lambda+2G}h'(z)\overline{h'(z)}\right\}|_{z=be^{i\theta}} \approx 2\left[\phi'(be^{i\theta}) + \overline{\phi'(be^{i\theta})}\right] \\
&\approx 2\left\{\left[\mu_0 H_0^2\left(\frac{b^2}{8Rt} - \frac{a^4 b^2 e^{2i\theta}}{4R^3 t^3}\right) + \frac{\mu_0 H_0^2 b^6}{4R^3 t^3}\frac{a^2}{b^2 e^{2i\theta}}\right] + \left[\mu_0 H_0^2\left(\frac{b^2}{8Rt} - \frac{a^4 b^2 e^{-2i\theta}}{4R^3 t^3}\right) + \frac{\mu_0 H_0^2 b^6}{4R^3 t^3}\frac{a^2}{b^2 e^{-2i\theta}}\right]\right\} \\
&\approx 2\frac{B_0^2}{\mu_0}\frac{R^2}{t^2}\cos(2\theta)
\end{aligned} \tag{104}$$

which is in accordance with that provided by Lin and Chen [12]. Notice that the radial stress t_{rr} is much small than $t_{\theta\theta}$ on the surface of cylindrical shell.

4.2. Ferromagnetic medium with a circular hole

In the present case, the regions S_a and S_b are air and S_c is made of a ferromagnetic material. Thus $\mu_{ra} = \mu_{rb} = 1$ and $\mu_{rc} \gg 1$ can be applied. The substitution of such data into Eqs. (12) and (20) yields $U_{ab} = U_{ba} = 1$, $V_{ab} = V_{ba} = 0$, $U_{bc} \approx 2$, $U_{cb} \approx 2/\mu_{rc} \ll 1$, $V_{bc} \approx 1$ and $V_{cb} \approx -1$. Thereafter, the ratio $H/H_0 \approx 2$ can be found. Furthermore, $G_a = G_b = 0$ can be taken for the air medium in S_a and S_b. And hence Eqs. (47) and (48) will result in $\Pi_{ab} = \Pi_{ba} = \Lambda_{ab} = \Lambda_{ba} = 0$ and $\Pi_{bc} = \Lambda_{bc} = -1$. Putting the above estimations into Eqs. (54)–(56), (A8) and (A9), taking $\mu_{rc} \gg 1$ for the ferromagnetic material on S_c and neglecting those terms which are much smaller than the dominant terms render

$$\begin{aligned}
&\phi_{cm}(z) \approx \mu_0\mu_{rc}^2 H_0^2\left(Tz - \overline{W}e^{2i\gamma}\frac{b^2}{z}\right), \quad \omega_{cm}(z) = \mu_0\mu_{rc}^2 H_0^2\left(We^{-2i\gamma}z - \overline{T}\frac{b^2}{z}\right), \\
&K, N_1, N_3 \sim \mu_0\mu_{rc}H_0^2
\end{aligned} \tag{105}$$

Applying Eqs. (28), (83), (103), (A19) and (A20), the magnetoelastic potential functions $\phi(z)$ and $\omega(z)$ on S_c can be obtained as

$$\phi(z) \approx \frac{B_0^2}{\mu_0}\left(Tz - \overline{W}e^{2i\gamma}\frac{b^2}{z}\right), \quad \omega(z) = \frac{B_0^2}{\mu_0}\left(We^{-2i\gamma}z - \overline{T}\frac{b^2}{z}\right) \quad z \in S_c \tag{106}$$

The corresponding $\psi(z)$ can be derived by the use of Eqs. (36), (84), (105), (106) and (A7) with the replacement of c by b in Eq. (36). It gives

$$\psi(z) = \omega(z) - \frac{b^2}{z}\phi'(z) = \frac{B_0^2}{\mu_0}\left(We^{-2i\gamma}z - \overline{T}\frac{b^2}{z}\right) - \frac{b^2}{z}\frac{B_0^2}{\mu_0}\left(T + \overline{W}\frac{b^2}{z^2}\right)$$
$$= \frac{B_0^2}{\mu_0}\left[\left(We^{-2i\gamma}z - \overline{T}\frac{b^2}{z}\right) - \frac{b^2}{z^2}\left(Tz + \overline{W}\frac{b^2}{z}\right)\right] \quad z \in S_c \tag{107}$$

This result is identical to that given by Lin [11] with $a = b$ and $\Gamma = \Gamma' = 0$ in Eqs. (4), (47), (48) and (71) of that paper.

5. Numerical results and discussion

The numerical results of this work are displayed with figures in this section to illustrate the influence of relevant parameters on the magnetoelastic stress fields. It is assumed that $\mu_{rb}/\mu_{ra} = \mu_{rb}/\mu_{rc}$, $G_b/G_a = G_b/G_c$ and $v_a = v_b = v_c = 0.3$ in the following paragraph. Furthermore, the magnetic induction progresses along x-axis (i.e. $\gamma = 0$) and the magnetoelastic stresses are expressed in a dimensionless form as divided with $B_0^2/2\mu_0$. Notice that the typical magnetic induction $B_0 = 1$ T (tesla) will induce the magnetic stress $B_0^2/2\mu_0 = 58$ psi (0.4 MPa). The variations of the dimensionless radial magnetoelastic stress $t_{rr}/\left(B_0^2/2\mu_0\right)$ and the dimensionless tangential magnetoelastic stress $t_{\theta\theta}/\left(B_0^2/2\mu_0\right)$ at point A are depicted in Fig. 2. The abscissa axis is presented with $\log_{10}$ scale and the values of relative magnetic permeability μ_{ra} and μ_{rc} are assumed to be 1 in this figure. Notice that the value of relative magnetic permeability for a ferromagnetic material, a paramagnetic material and a diamagnetic material is much greater than 1, slightly greater than 1 and slightly less than 1, respectively. Therefore, the extent of the ratio $\mu_{rb}/\mu_{ra}(=\mu_{rb}/\mu_{rc})$ in Fig. 2 is taken to be higher that 1 from practical point of view. As shown in Fig. 1, the point A is located on the surface of region S_b with $\theta = 0$. Thus the radial magnetoelastic stress $t_{rr}/\left(B_0^2/2\mu_0\right)$ is this figure

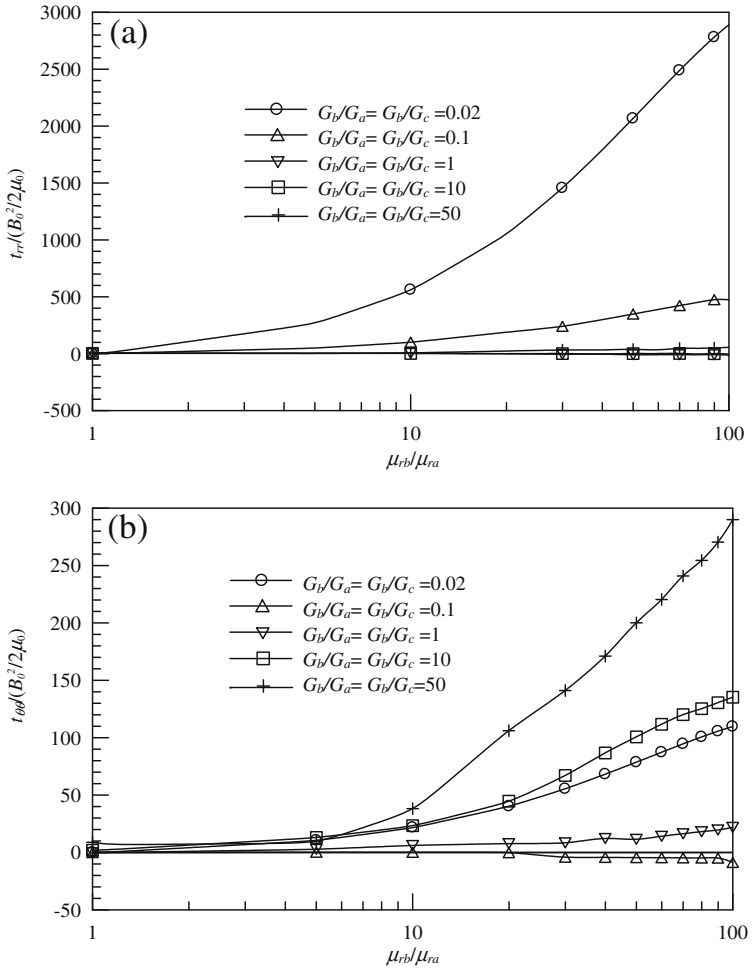

Fig. 2. The variations of dimensionless magnetoelastic stresses at point A with respect to the ratio of magnetic susceptibility μ_{rb}/μ_{ra} under $\mu_{ra} = \mu_{rc} = 1$, $b/a = 1.01$ (a) $t_{rr}/\left(B_0^2/2\mu_0\right)$ (b) $t_{\theta\theta}/\left(B_0^2/2\mu_0\right)$.

can be regarded as the interfacial normal stress between the regions S_b and S_c. Since the point A falls on the x-axis which is the symmetric line of the region S_b for the present case with $\gamma = 0$, the interfacial shear stress $t_{r\theta}/\left(B_0^2/2\mu_0\right)$ at point A equals zero. It is observed from Fig. 2 that higher $G_b/G_a(=G_b/G_c)$ ratio will cause lower values of the magnetoelastic stresses $t_{rr}/\left(B_0^2/2\mu_0\right)$ and $t_{\theta\theta}/\left(B_0^2/2\mu_0\right)$ when the ratio $G_b/G_a(=G_b/G_c) < 0.1$. Once the ratio $G_b/G_a(=G_b/G_c) > 1$, higher $G_b/G_a(=G_b/G_c)$ ratio may induce higher values of the magnetoelastic stresses $t_{rr}/\left(B_0^2/2\mu_0\right)$ and $t_{\theta\theta}/\left(B_0^2/2\mu_0\right)$. In the intermediate region $1 > G_b/G_a(=G_b/G_c) > 0.1$, the variation of the magnetoelastic stresses are not significant. The above observation denotes that the difference of the magnetic property G between the region S_a (or S_c) and the region S_b may cause higher value of the radial and the tangential magnetoelastic stresses. Furthermore, when the ratio $\mu_{rb}/\mu_{ra}(=\mu_{rb}/\mu_{rc})$ moves from 1 to a higher value, the magnetoelastic stresses also increase. This means that the difference of the magnetic property μ_r between the region S_a(or S_c) and the region S_b may evoke the rising of the radial and the tangential magnetoelastic stresses. From Fig. 2a, the value of the dimensionless radial magnetoelastic stress $t_{rr}/\left(B_0^2/2\mu_0\right)$ with $\mu_{rb}/\mu_{ra}(=\mu_{rb}/\mu_{rc}) = 50$ and G_b/G_a (or G_b/G_c) = 0.02 is found to be 2000. From the above estimation of $B_0^2/2\mu_0 = 0.4$ MPa under the applied magnetic induction $B_0 = 1$ T, this value corresponds to 800 MPa of real radial stress at point A. For practical application, such a stress level is considerable for stainless steel (AISI 302) with tensile strength of 860 MPa. On the other hand, the dimensionless tangential magnetoelastic stress $t_{\theta\theta}/\left(B_0^2/2\mu_0\right)$ with $\mu_{rb}/\mu_{ra}(=\mu_{rb}/\mu_{rc}) = 100$ and G_b/G_a (or G_b/G_c) = 50 equals 288. Such a value is corresponding to 860 MPa of real tangential stress at point A under the applied magnetic induction $B_0 = 2.73$ T. Thus the tangential stress at point A is over the tensile strength of stainless steel once the strength of applied magnetic induction B_0 is greater than 2.73 T. This is the critical value of the applied magnetic induction for the present condition with S_b made of stainless steel. Inside a toroidal magnetic fusion reactor, there is a large magnetic induction (>5 T). From the point of view for practical application, the magnetoelastic stresses inside the intermediate region S_b of a three-phase composite cylinder become dominant when the ratios μ_{rb}/μ_{ra} (or μ_{rb}/μ_{rc}) and G_b/G_a (or G_b/G_c) increase over a certain value. Thus the failure analysis and prevention of the composite structure with higher μ_{rb}/μ_{ra} (or μ_{rb}/μ_{rc}) and G_b/G_a (or G_b/G_c) ratios need to be considered, especially for a structure under an environment with strong magnetic induction.

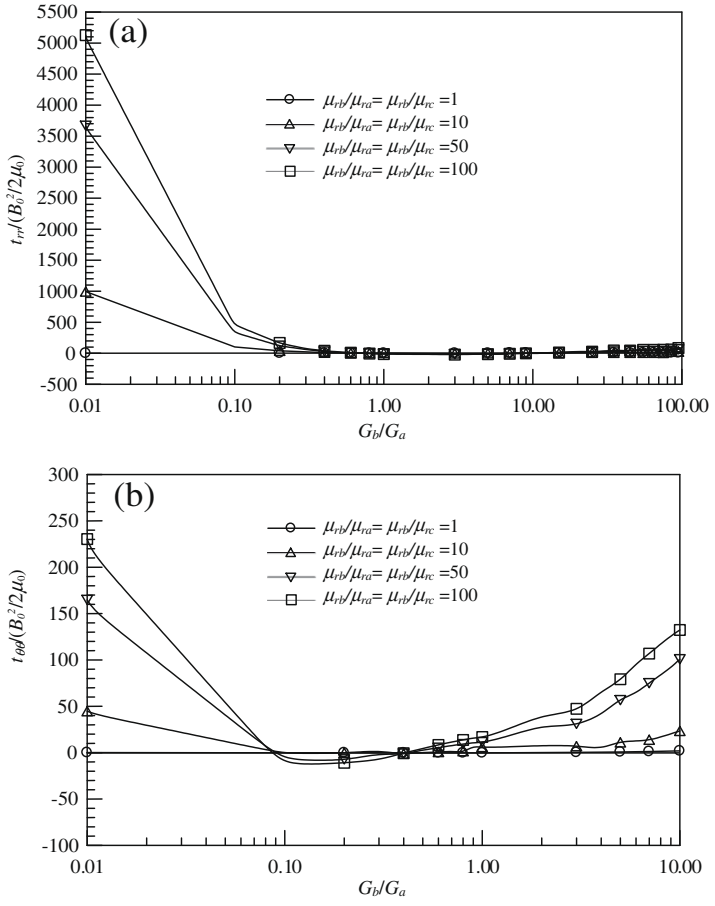

Fig. 3. The variations of dimensionless magnetoelastic stresses at point A with respect to the ratio of shear modulus G_b/G_a under $G_a = G_c$, $\mu_{ra} = \mu_{rc} = 1$ and $b/a = 1.01$ (a) $t_{rr}/\left(B_0^2/2\mu_0\right)$ (b) $t_{\theta\theta}/\left(B_0^2/2\mu_0\right)$.

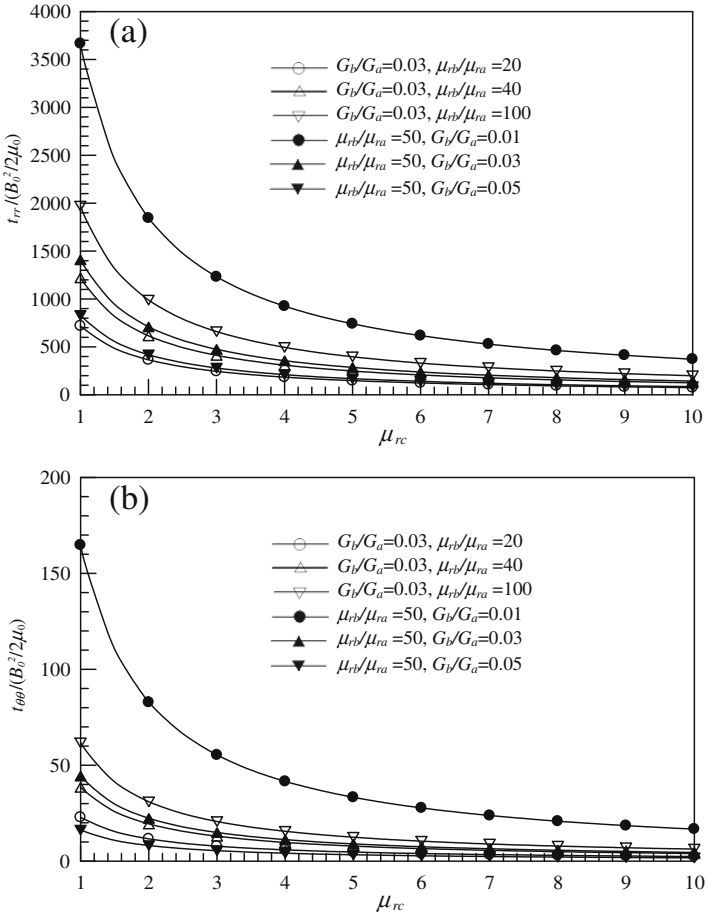

Fig. 4. The variations of dimensionless magnetoelastic stresses at point A with respect to the magnetic susceptibility μ_{rc} under $G_a = G_c$, $\mu_{ra} = \mu_{rc}$ and b/a = 1.01 (a) $t_{rr}/\left(B_0^2/2\mu_0\right)$ (b) $t_{\theta\theta}/\left(B_0^2/2\mu_0\right)$.

Fig. 3 displays the variations of the dimensionless magnetoelastic stresses $t_{rr}/\left(B_0^2/2\mu_0\right)$ and $t_{\theta\theta}/\left(B_0^2/2\mu_0\right)$ at point A with respect to the ratio $G_b/G_a(=G_b/G_a)$ under b/a = 1.01 and various $\mu_{rb}/\mu_{ra}(=\mu_{rb}/\mu_{rc})$ values. The abscissa axis in Fig. 3 is also depicted with $\log_{10}$ scale as that adopted in Fig. 2. From Fig. 3, the feature that the magnetoelastic stress $t_{rr}/\left(B_0^2/2\mu_0\right)$ increases with the increase of $\mu_{rb}/\mu_{ra}(=\mu_{rb}/\mu_{rc})$ can be found. Except for the curve with $\mu_{rb}/\mu_{ra}(=\mu_{rb}/\mu_{rc}) = 1$, which leads to very small $t_{rr}/\left(B_0^2/2\mu_0\right)$, the other curves in Fig. 3a reveal that the magnetoelastic stress $t_{rr}/\left(B_0^2/2\mu_0\right)$ increases with the ratio $G_b/G_a(=G_b/G_c)$ when this ratio is less then 1. Once the ratio $G_b/G_a(=G_b/G_c)$ is greater than 1, the variation of the magnetoelastic stress $t_{rr}/\left(B_0^2/2\mu_0\right)$ on this ratio becomes insignificant. The curve in Fig. 3b with $\mu_{rb}/\mu_{ra}(=\mu_{rb}/\mu_{rc}) = 1$ also has very small $t_{\theta\theta}/\left(B_0^2/2\mu_0\right)$ and the magnetoelastic stress $t_{\theta\theta}/(B_0^2/2\mu_0)$ of the other curves decrease with the increase of ratio $G_b/G_a(=G_b/G_c)$ for $G_b/G_a < 0.1$ and increase with the ratio G_b/G_a for further increase of this ratio. It is interpreted that the materials in S_a and S_c with higher stiffness than that in S_b may provide stronger restriction on the deformation of annular region S_b and may cause higher interfacial radial stress and tangential stress. On the other hand, the material in S_b can extend and induce higher tangential stress while its stiffness becomes much higher than that in S_a and S_c. With $\mu_{rb}/\mu_{ra}(=\mu_{rb}/\mu_{rc}) = 50$ and G_b/G_a (or G_b/G_c) = 0.01, the dimensionless magnetoelastic stresses $t_{rr}/\left(B_0^2/2\mu_0\right)$ and $t_{\theta\theta}/\left(B_0^2/2\mu_0\right)$ are found to be 3600 and 160, respectively. Such results lead to the real magnetoelastic stress t_{rr} = 12,960 MPa with B_0 = 1 T and $t_{\theta\theta}$ = 860 MPa with B_0 = 3.665 T. Such values of magnetoelastic stresses are considerable in the practical application as mentioned above. The value of 860 MPa equals the tensile strength of stainless steel (AISI 302). Therefore, the value 3.665 T of B_0 can be viewed as the critical value for the present condition with S_b made of stainless steel.

The variations of the dimensionless magnetoelastic stresses $t_{rr}/\left(B_0^2/2\mu_0\right)$ and $t_{\theta\theta}/\left(B_0^2/2\mu_0\right)$ at point A on the relative magnetic permeability $\mu_{rc}(=\mu_{ra})$ with b/a = 1.01 under various $\mu_{rb}/\mu_{ra}(=\mu_{rb}/\mu_{rc})$ and $G_b/G_a(=G_b/G_c)$ ratios are presented in Fig. 4. One can find that both the magnetoelastic stresses decrease with the increase of μ_{rc}. Furthermore, the magnetoelastic stresses also increase with the ratio μ_{rb}/μ_{ra} under a fixed value of G_b/G_a and decrease with the increase of ratio $G_b/G_a(<1)$ under a fixed value of μ_{rb}/μ_{ra}. This results are consistent with Figs. 2 and 3 that the difference of material properties μ_r and G in S_a

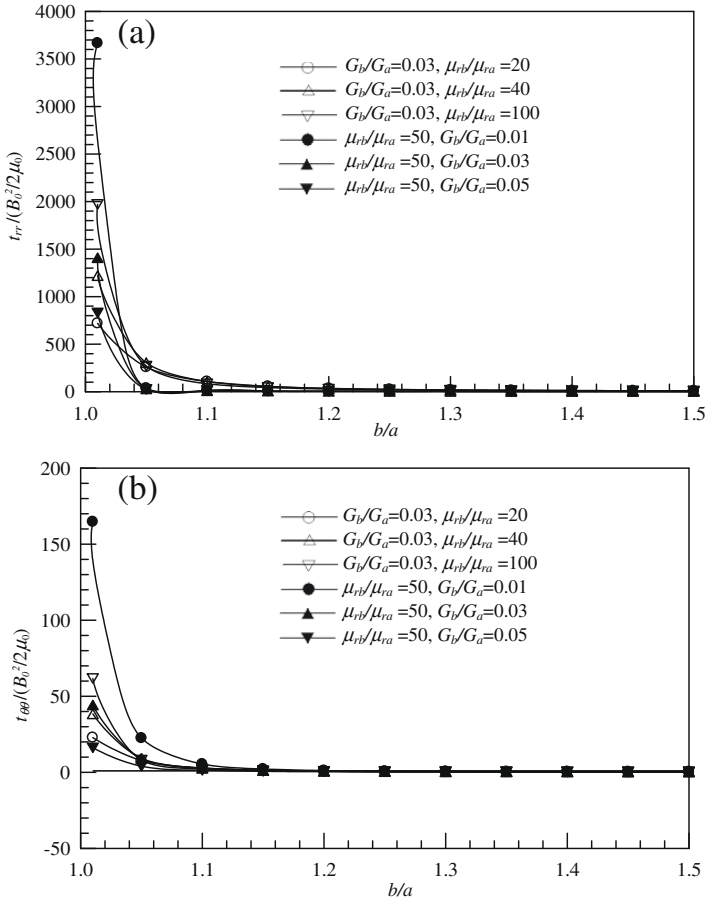

Fig. 5. The variations of dimensionless magnetoelastic stresses at point A with respect to the ratio b/a under $G_a = G_c$, $\mu_{ra} = \mu_{rc} = 1$ (a) $t_{rr}/\left(B_0^2/2\mu_0\right)$ (b) $t_{\theta\theta}/\left(B_0^2/2\mu_0\right)$.

(or S_c) and S_b may evoke the raise of the magnetoelastic stress on the interface. Fig. 5 depicts the variation of the dimensionless magnetoelastic stresses $t_{rr}/\left(B_0^2/2\mu_0\right)$ and $t_{\theta\theta}/\left(B_0^2/2\mu_0\right)$ at point A with respect to the radius ratio b/a under various $\mu_{rb}/\mu_{ra}(=\mu_{rb}/\mu_{rc})$ and $G_b/G_a(=G_b/G_c)$ ratios. It is observed that both the magnetoelastic stresses decrease with the increase of b/a ratio. This means that thicker intermediate region S_b under a fixed radius a will reduce the magnetoelastic stresses at point A on the interface. In analogy to Fig. 4, the magnetoelastic stresses increase with the ratio μ_{rb}/μ_{ra} under a fixed value of G_b/G_a and decrease with the increase of ratio $G_b/G_a(<1)$ under a fixed value of μ_{rb}/μ_{ra} can be also found from Fig. 5. The estimation of the real magnetoelastic stresses corresponding to the dimensionless stresses in Figs. 4 and 5 are similar to that provided in the previous paragraph for Fig. 3.

The variations of the dimensionless magnetoelastic stresses $t_{rr}/\left(B_0^2/2\mu_0\right), t_{\theta\theta}/\left(B_0^2/2\mu_0\right)$ and $t_{r\theta}/\left(B_0^2/2\mu_0\right)$ with respect to the circumference angle θ under $\mu_{ra} = \mu_{rc} = 1$, $b/a = 1.01$ and various $\mu_{rb}/\mu_{ra}(=\mu_{rb}/\mu_{rc})$ and $G_b/G_a(=G_b/G_c)$ ratios are depicted in Fig. 6. It is found from this figure that the curves possess period π(or 180°). This result can be interpreted as that the expressions of $\phi(z)$ and $\omega(z)$ on S_b in Eqs. (83) and (84) with Eqs. (100), (101), (A17) and (A18) have dominant terms of z^3, z and z^{-1} for the present case. The derivatives of such terms become z^2, z^0 and z^{-2}, respectively and hence the magnetoelastic stresses in Eqs. (32) and (37) have period π. The values of the magnetoelastic stresses $t_{rr}/\left(B_0^2/2\mu_0\right)$ and $t_{\theta\theta}/\left(B_0^2/2\mu_0\right)$ in Fig. 6 increase with the ratio μ_{rb}/μ_{ra} under a fixed value of G_b/G_a and decrease with the increase of ratio $G_b/G_a(<1)$ under a fixed value of μ_{rb}/μ_{ra} in accordance with Fig. 5. Furthermore, the values of magnetoelastic stress $t_{r\theta}/\left(B_0^2/2\mu_0\right)$ at $\theta = 0$ equal zero in this figure. Such a result guarantees that $t_{r\theta}/\left(B_0^2/2\mu_0\right)$ at point A vanishes as mentioned above. The estimation of the real magnetoelastic stresses corresponding to the dimensionless stresses in Fig. 6 are also similar to that provided in the previous paragraph for Fig. 3.

From the estimation of the real magnetoelastic stresses in the illustrated case of Figs. 2–6, it is concluded that the applied uniform magnetic induction may evoke significant magnetoelastic stresses on a three-phase composite cylinder with higher values of the $G_b/G_a(=G_b/G_c)$, $\mu_{rb}/\mu_{ra}(=\mu_{rb}/\mu_{rc})$ ratios and lower values of the $\mu_{ra}(=\mu_{rc})$, b/a ratio. Here the higher values of the $G_b/G_a(=G_b/G_c)$ and $\mu_{rb}/\mu_{ra}(=\mu_{rb}/\mu_{rc})$ ratios denote the deviation of the material properties between different phases becomes larger. By comparing the stresses of this study with the tensile strength of real material, such as stainless steel, the critical value of the applied magnetic induction can be obtained. From the practical point of view, such estimations that reveal the effect of various parameters on the real magnetoelastic stresses are necessary.

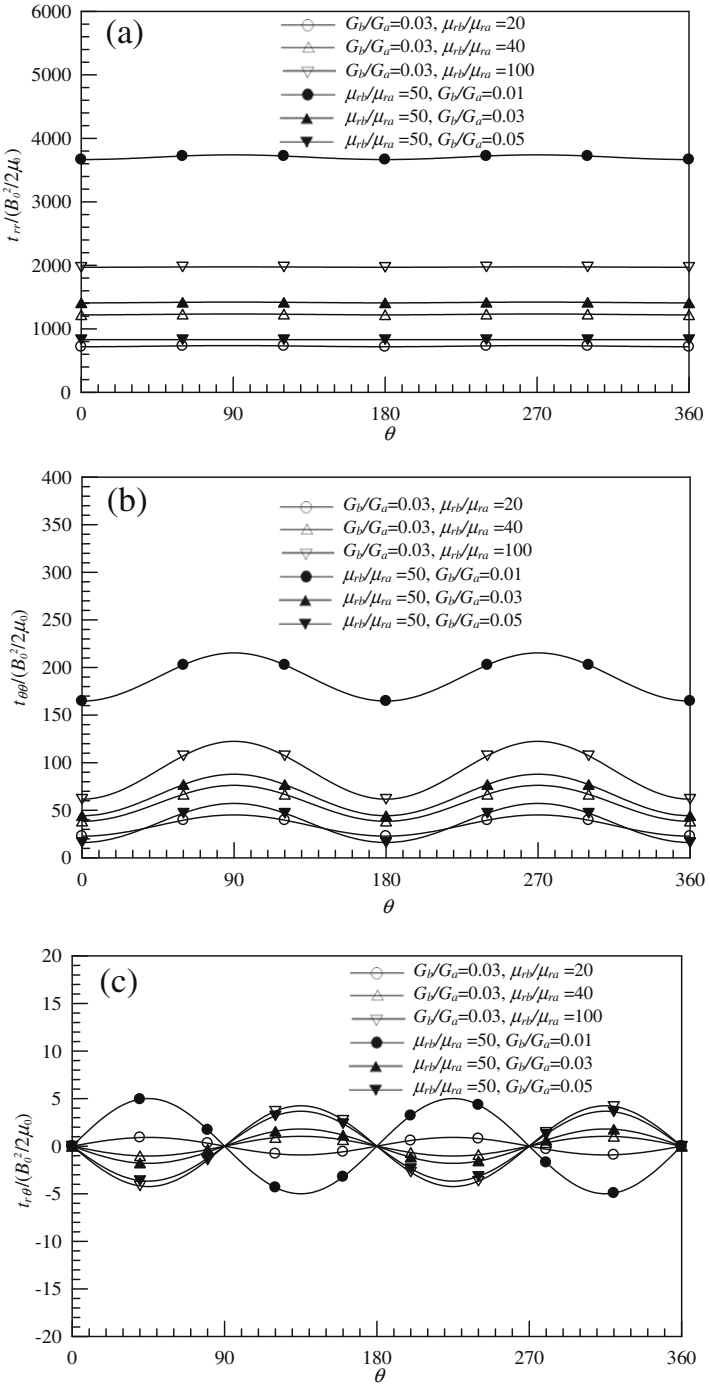

Fig. 6. The variations of dimensionless magnetoelastic stresses with respect to the circumference angle θ under $\mu_{ra} = \mu_{rc} = 1$, $b/a = 1.01$ (a) $t_{rr}/\left(B_0^2/2\mu_0\right)$ (b) $t_{\theta\theta}/\left(B_0^2/2\mu_0\right)$ (c) $t_{r\theta}/\left(B_0^2/2\mu_0\right)$.

6. Conclusions

By applying the alternating technique and the method of analytical continuation on the complex form of magnetoelasticity, the magnetic and the magnetoelastic fields on a three-phase composite cylinder subjected to a remote uniform magnetic induction are derived in this paper. It is noted that the boundary conditions at both interfaces between three phases can be satisfied subsequently. Thus the solutions of complex potential functions can be expressed in a series form. With the typical data of material properties, the series solutions are found to be convergent and then tend to the exact solutions. The numerical illustrations of magnetoelastic stresses at outer face of intermediate phase are shown with figures to present the effects of various parameters. Furthermore, the estimations of real magnetoelastic stresses corresponding to the dimensionless results in the illustrated figures are provided and compared with the strength of real material data to make the present study meaningful in practical application. By comparing the results of this study with the literature under special cases, such as cylindrical shell in vacuum and an infinite matrix with a circular hole, the correctness of this work can be guaranteed.

Acknowledgements

The authors would like to thank the financial support by the National Science Council, ROC through Grant No. NSC 98-2221-E-240-003.

Appendix A. The solving process of $\phi_{bm}(z)$, $\omega_{bm}(z)$, $\phi_{cm}(z)$ and $\omega_{bm}(z)$

By applying analytic continuation across the interface L, it is found from Eqs. (39) and (40) that

$$\begin{aligned}&\phi_{bm}(z)-\overline{\omega_{cm}}\left(\frac{b^2}{z}\right)+\frac{G_b\mu_0\chi_b}{\lambda_b+2G_b}H^2\left[\left(1-V_{ab}^2\frac{a^4}{b^4}\right)z-V_{ab}e^{-2i\gamma}\frac{a^2}{b^4}z^3\right]-\frac{\mu_0(\mu_{rb}+\chi_b)}{2}H^2V_{ab}\frac{a^2}{b^2}\left(2z-\frac{V_{ab}}{3}\frac{a^2}{b^4}e^{-2i\gamma}z^3\right)\\&-\frac{G_c\mu_0\chi_c}{\lambda_c+2G_c}H_0^2\left\{\left[1-\left(V_{bc}+U_{cb}V_{ab}\frac{H}{H_0}\frac{a^2}{b^2}\right)^2\right]z-\left(V_{bc}+U_{cb}V_{ab}\frac{H}{H_0}\frac{a^2}{b^2}\right)e^{-2i\gamma}\frac{z^3}{b^2}\right\}\\&+\frac{\mu_0(\mu_{rc}+\chi_c)}{2}H_0^2\left[\left(V_{bc}+U_{cb}V_{ab}\frac{H}{H_0}\frac{a^2}{b^2}\right)\left(2z-\frac{e^{2i\gamma}}{3}\frac{z^3}{b^2}\right)+C_{bm}z-\mu_0\mu_{rc}^2H_0^2Tz+\mu_0\mu_{rc}^2H_0^2\overline{W}e^{2i\gamma}\frac{b^2}{z}=0\quad z\in S_a\cup S_b\right.\end{aligned}\tag{A1}$$

$$\begin{aligned}&\phi_{cm}(z)-\overline{\omega_{bm}}\left(\frac{b^2}{z}\right)-\left\{\left[\frac{G_b\mu_0\chi_b}{\lambda_b+2G_b}V_{ab}\frac{a^2}{b^2}-\frac{\mu_0(\mu_{rb}+\chi_b)}{2}\right]\left(\frac{H}{H_0}\right)^2\right.\\&\left.-\left[\frac{G_c\mu_0\chi_c}{\lambda_c+2G_c}\left(V_{bc}+U_{cb}V_{ab}\frac{H}{H_0}\frac{a^2}{b^2}\right)-\frac{\mu_0(\mu_{rc}+\chi_c)}{2}\right]\right\}H_0^2e^{2i\gamma}\frac{b^2}{z}+C_{bm}z-\mu_0\mu_{rc}^2H_0^2Tz+\mu_0\mu_{rc}^2H_0^2\overline{W}e^{2i\gamma}\frac{b^2}{z}=0\quad z\in S_c\end{aligned}\tag{A2}$$

$$\begin{aligned}&\frac{\kappa_b\phi_{bm}(z)}{2G_b}+\frac{\overline{\omega_{cm}}\left(\frac{b^2}{z}\right)}{2G_c}-\frac{\mu_0}{2}\left\{\frac{\chi_bH^2}{\lambda_b+2G_b}\left(1-V_{ab}^2\frac{a^4}{b^4}\right)-\frac{\chi_cH_0^2}{\lambda_c+2G_c}\left[1-\left(V_{bc}+U_{cb}V_{ab}\frac{H}{H_0}\frac{a^2}{b^2}\right)^2\right]\right\}z\\&+\frac{\mu_0}{2}\left[\frac{\chi_bH^2V_{ab}}{\lambda_b+2G_b}\frac{a^2}{b^2}-\frac{\chi_cH_0^2}{\lambda_c+2G_c}\left(V_{bc}+U_{cb}V_{ab}\frac{H}{H_0}\frac{a^2}{b^2}\right)\right]e^{-2i\gamma}\frac{z^3}{b^2}-\frac{C_{bm}z}{2G_b}\\&-\frac{\kappa_c}{2G_c}\mu_0\mu_{rc}^2H_0^2Tz-\frac{\mu_0\mu_{rc}^2H_0^2\overline{W}e^{2i\gamma}}{2G_c}\frac{b^2}{z}=0\quad z\in S_a\cup S_b\end{aligned}\tag{A3}$$

$$\begin{aligned}&\frac{\kappa_c\phi_{cm}(z)}{2G_c}+\frac{\overline{\omega_{bm}}\left(\frac{b^2}{z}\right)}{2G_b}+\frac{\mu_0}{2}\left[\frac{\chi_bH^2V_{ab}}{\lambda_b+2G_b}\frac{a^2}{b^2}-\frac{\chi_cH_0^2}{\lambda_c+2G_c}\left(V_{bc}+U_{cb}V_{ab}\frac{H}{H_0}\frac{a^2}{b^2}\right)\right]e^{2i\gamma}\frac{b^2}{z}-\frac{\kappa_cS}{2G_c}-\frac{\overline{T}}{2G_c}\frac{b^2}{z}\\&-\frac{C_{bm}z}{2G_b}-\frac{\kappa_c}{2G_c}\mu_0\mu_{rc}^2H_0^2Tz-\frac{\mu_0\mu_{rc}^2H_0^2\overline{W}e^{2i\gamma}}{2G_c}\frac{b^2}{z}=0\quad z\in S_c\end{aligned}\tag{A4}$$

where

$$C_{bm}=\overline{\phi'_{bm}}(0),H=\frac{U_{bc}H_0}{1-\frac{a^2}{b^2}V_{cb}V_{ab}},T=\frac{1}{2}\left(\frac{1}{4}-\frac{\chi_c}{\mu_{rc}^2}\right),W=\frac{1}{2}\left(\frac{1}{2}-\frac{\mu_{rc}+\chi_c}{\mu_{rc}^2}\right)\tag{A5}$$

The symbol H, which is introduced for the sake of convenience, can make the expression in the derivation process more compact. Solving Eqs. (A1)–(A4), one can obtain

$$\begin{aligned}\phi_{bm}(z)=\mu_0H_0^2\Bigg\{&\frac{1}{1-\Pi_{cb}}\left[\frac{\chi_b\Pi_{cb}G_b}{\lambda_b+2G_b}\frac{H^2}{H_0^2}\left(1-V_{ab}^2\frac{a^4}{b^4}\right)+\frac{G_b(\mu_{rb}+\chi_b)V_{ab}}{G_b+\kappa_bG_c}\frac{H^2}{H_0^2}\frac{a^2}{b^2}-\frac{G_b(\mu_{rc}+\chi_c)}{G_b+\kappa_bG_c}\left(V_{bc}+U_{cb}V_{ab}\frac{H}{H_0}\frac{a^2}{b^2}\right)\right.\\&\left.+(1-\Pi_{cb})(1+\Lambda_{bc})\mu_{rc}^2T\right]z-\left[\frac{\chi_b\Pi_{cb}G_bV_{ab}e^{-2i\gamma}}{\lambda_b+2G_b}\frac{H^2}{H_0^2}\frac{a^4}{b^4}+\frac{G_b(\mu_{rb}+\chi_b)V_{ab}^2e^{-2i\gamma}}{6(G_b+\kappa_bG_c)}\frac{H^2}{H_0^2}\frac{a^6}{b^6}-\frac{G_b(\mu_{rc}+\chi_c)e^{2i\gamma}}{6(G_b+\kappa_bG_c)}\right.\\&\left.\times\left(V_{bc}+U_{cb}V_{ab}\frac{H}{H_0}\frac{a^2}{b^2}\right)^2\frac{a^2}{b^2}\right]\frac{z^3}{a^2}\Bigg\}\quad z\in S_a\cup S_b\end{aligned}\tag{A6}$$

$$\begin{aligned}\omega_{bm}(z)=\mu_0H_0^2\Bigg\{&\frac{\chi_bG_b}{\lambda_b+2G_b}\frac{H^2}{H_0^2}\left[\frac{\Pi_{cb}}{1-\Pi_{cb}}\left(1-V_{ab}^2\frac{a^4}{b^4}\right)-V_{ab}e^{-2i\gamma}\frac{a^2}{b^2}\right]+G_b(\mu_{rb}+\chi_b)\frac{H^2}{H_0^2}\left[\frac{\kappa_ce^{-2i\gamma}}{2(G_c+\kappa_cG_b)}+\frac{V_{ab}}{G_b+\kappa_bG_c}\frac{a^2}{b^2}\right]\\&+\frac{\chi_cG_c(1+\Pi_{bc})}{\lambda_c+2G_c}\left(V_{bc}+U_{cb}V_{ab}\frac{H}{H_0}\frac{a^2}{b^2}\right)-G_b(\mu_{rc}+\chi_c)\left[\frac{\kappa_ce^{-2i\gamma}}{2(G_c+\kappa_cG_b)}+\frac{1}{G_b+\kappa_bG_c}\left(V_{bc}+U_{cb}V_{ab}\frac{H}{H_0}\frac{a^2}{b^2}\right)\right]\\&+(1+\Pi_{bc})\mu_{rc}^2We^{-2i\gamma}\Bigg\}z\quad z\in S_a\cup S_b\end{aligned}\tag{A7}$$

$$\phi_{cm}(z)=\mu_0H_0^2\left\{e^{2i\gamma}\left[-\frac{\mu_{rb}+\chi_b}{2}\frac{G_c}{G_c+\kappa_cG_b}\frac{H^2}{H_0^2}+\frac{\chi_c\Pi_{bc}G_c}{\lambda_c+2G_c}\left(V_{bc}+U_{cb}V_{ab}\frac{H}{H_0}\frac{a^2}{b^2}\right)\right.\right.$$
$$\left.\left.+\frac{\mu_{rc}+\chi_c}{2}\frac{G_c}{G_c+\kappa_cG_b}+\Pi_{bc}\mu_{rc}^2\overline{W}\right]\frac{b^2}{z}+\mu_{rc}^2Tz\right\}\quad z\in S_c \tag{A8}$$

$$\omega_{cm}(z)=\frac{\mu_0H_0^2\kappa_bG_c}{G_b+\kappa_bG_c}\left\{\left[\frac{(1+\Pi_{cb})\chi_bG_b(G_b+\kappa_bG_c)}{G_c\kappa_b(\lambda_b+2G_b)}\frac{H^2}{H_0^2}\left(1-V_{ab}^2\frac{a^4}{b^4}\right)-(\mu_{rb}+\chi_b)V_{ab}\frac{H^2}{H_0^2}\frac{a^2}{b^2}-\frac{\chi_c(G_b+\kappa_bG_c)}{\kappa_b(\lambda_c+2G_c)}\right.\right.$$
$$+\frac{\chi_c(G_b+\kappa_bG_c)}{\kappa_b(\lambda_c+2G_c)}\left(V_{bc}+U_{cb}V_{ab}\frac{H}{H_0}\frac{a^2}{b^2}\right)^2+(\mu_{rc}+\chi_c)\left(V_{bc}+U_{cb}V_{ab}\frac{H}{H_0}\frac{a^2}{b^2}\right)+\left.\frac{(G_b+\kappa_bG_c)\Lambda_{bc}\mu_{rc}^2\overline{T}}{\kappa_bG_c}\right]\frac{b^2}{z}$$
$$-\frac{1}{6}\left[\frac{6\chi_bG_b(G_b+\kappa_bG_c)(1+\Pi_{cb})V_{ab}e^{2i\gamma}}{\kappa_bG_c(\lambda_b+2G_b)}\frac{H^2}{H_0^2}\frac{a^2}{b^2}-(\mu_{rb}+\chi_b)V_{ab}^2e^{-2i\gamma}\frac{H^2}{H_0^2}\frac{a^4}{b^4}\right.$$
$$+\left(\mu_{rc}+\chi_c\right)e^{-2i\gamma}\left(V_{bc}+U_{cb}V_{ab}\frac{H}{H_0}\frac{a^2}{b^2}\right)+\frac{\chi_c(G_b+\kappa_bG_c)e^{2i\gamma}}{\kappa_b(\lambda_c+2G_c)}\left(V_{bc}+U_{cb}V_{ab}\frac{H}{H_0}\frac{a^2}{b^2}\right)\Big]\frac{b^4}{z^3}$$
$$+\frac{(G_b+\kappa_bG_c)(1+\Pi_{cb})}{\kappa_bG_c(1-\Pi_{cb})}\left[\frac{\Pi_{cb}\chi_bG_b}{\lambda_b+2G_b}\frac{H^2}{H_0^2}\left(1-V_{ab}^2\frac{a^4}{b^4}\right)+\frac{G_b(\mu_{rb}+\chi_b)V_{ab}}{G_b+\kappa_bG_c}\frac{H^2}{H_0^2}\frac{a^2}{b^2}\right.$$
$$\left.\left.-\frac{G_b(\mu_{rc}+\chi_c)}{G_b+\kappa_bG_c}\left(V_{bc}+U_{cb}V_{ab}\frac{H}{H_0}\frac{a^2}{b^2}\right)+\frac{1-\Pi_{cb}}{1+\Pi_{cb}}\mu_{rc}^2We^{-2i\gamma}\right]z\right\}\quad z\in S_c \tag{A9}$$

Appendix B. The solving process of $\phi_{am}(z)$, $\omega_{am}(z)$, $\phi_{b0}(z)$ and $\omega_{b0}(z)$

Applying the analytic continuation on Eqs. (49) and (50) and using Eqs. (47), (48), (A6) and (A7) yield

$$\phi_{am}(z)-\phi_{bm}(z)-\overline{\omega_{b0}}\left(\frac{a^2}{z}\right)+\frac{G_a\mu_0\chi_aU_{ab}^2H^2}{\lambda_a+2G_a}z-(1+\Lambda_{bc})\mu_0\mu_{rc}^2H_0^2Tz-\frac{G_b\mu_0\chi_bH^2}{\lambda_b+2G_b}\left[(1-V_{ab}^2)z-V_{ab}e^{-2i\gamma}\frac{z^3}{a^2}\right]$$
$$-\frac{\mu_0(a^2-b^2)}{1-\Pi_{cb}}\left\{\frac{\chi_bG_b\Pi_{cb}H^2}{\lambda_b+2G_b}\left(1-V_{ab}^2\frac{a^4}{b^4}\right)+\frac{G_b}{G_b+\kappa_bG_c}\left[(\mu_{rb}+\chi_b)H^2V_{ab}\frac{a^2}{b^2}-(\mu_{rc}+\chi_c)H_0^2\left(V_{bc}+U_{cb}V_{ab}\frac{H}{H_0}\frac{a^2}{b^2}\right)\right]\right\}\frac{z}{a^2}$$
$$+\frac{\mu_0(\mu_{rb}+\chi_b)H^2V_{ab}}{2}\left(2z-\frac{V_{ab}e^{-2i\gamma}}{3}\frac{z^3}{a^2}\right)+C_{am}z=0\quad z\in S_a \tag{A10}$$

$$\phi_{b0}(z)+\overline{\omega_{bm}}\left(\frac{a^2}{z}\right)-\overline{\omega_{am}}\left(\frac{a^2}{z}\right)+\left[\frac{(\mu_{ra}+\chi_a)U_{ab}^2}{2}+\frac{G_b\mu_0\chi_bV_{ab}}{\lambda_b+2G_b}\right]\mu_0H^2e^{2i\gamma}\frac{a^2}{z}+(1+\Pi_{bc})\mu_0\mu_{rc}^2H_0^2\overline{W}e^{2i\gamma}\frac{a^2}{z}$$
$$-\frac{\mu_0(a^2-b^2)}{1-\Pi_{cb}}\left\{\frac{3\chi_bG_b\Pi_{cb}H^2V_{ab}e^{2i\gamma}}{\lambda_b+2G_b}\frac{a^4}{b^4}+\frac{G_b}{2(G_b+\kappa_bG_c)}\left[(\mu_{rb}+\chi_b)H^2V_{ab}^2e^{2i\gamma}\frac{a^6}{b^6}\right.\right.$$
$$\left.\left.-(\mu_{rc}+\chi_c)H_0^2e^{-2i\gamma}\left(V_{bc}+U_{cb}V_{ab}\frac{H}{H_0}\frac{a^2}{b^2}\right)^2\frac{a^2}{b^2}\right]\right\}\frac{1}{z}-\frac{\mu_0(\mu_{rb}+\chi_b)H^2e^{2i\gamma}}{2}\frac{a^2}{z}+C_{am}z=0\quad z\in S_b\cup S_c \tag{A11}$$

$$\frac{\kappa_a\phi_{am}(z)}{2G_a}-\frac{\kappa_b\phi_{bm}(z)}{2G_b}+\frac{\overline{\omega_{b0}}\left(\frac{a^2}{z}\right)}{2G_b}-\frac{\mu_0\chi_aU_{ab}^2H^2}{2(\lambda_a+2G_a)}z-\frac{\kappa_b(1+\Lambda_{bc})\mu_0\mu_{rc}^2H_0^2T}{2G_b}z+\frac{\mu_0\chi_bH^2}{2(\lambda_b+2G_b)}\left[(1-V_{ab}^2)z-V_{ab}e^{-2i\gamma}\frac{z^3}{a^2}\right]$$
$$+\frac{\mu_0(a^2-b^2)}{2G_b(1-\Pi_{cb})}\left\{\frac{\chi_bG_b\Pi_{cb}H^2}{\lambda_b+2G_b}\left(1-V_{ab}^2\frac{a^4}{b^4}\right)+\frac{G_b}{G_b+\kappa_bG_c}\right.$$
$$\left.\times\left[(\mu_{rb}+\chi_b)H^2V_{ab}\frac{a^2}{b^2}-(\mu_{rc}+\chi_c)H_0^2\left(V_{bc}+U_{cb}V_{ab}\frac{H}{H_0}\frac{a^2}{b^2}\right)\right]\right\}\frac{z}{a^2}-\frac{C_{am}}{2G_a}z=0\quad z\in S_a \tag{A12}$$

$$\frac{\kappa_b\phi_{b0}(z)}{2G_b}-\frac{\overline{\omega_{bm}}\left(\frac{a^2}{z}\right)}{2G_b}+\frac{\overline{\omega_{am}}\left(\frac{a^2}{z}\right)}{2G_a}-\frac{(1+\Pi_{bc})\mu_0\mu_{rc}^2H_0^2\overline{W}e^{2i\gamma}}{2G_b}\frac{a^2}{z}-\frac{\mu_0\chi_bH^2V_{ab}e^{2i\gamma}}{2(\lambda_b+2G_b)}\frac{a^2}{z}$$
$$-\frac{\mu_0(a^2-b^2)}{2G_b(1-\Pi_{cb})}\left\{\frac{3\chi_bG_b\Pi_{cb}H^2V_{ab}e^{2i\gamma}}{\lambda_b+2G_b}\frac{a^4}{b^4}+\frac{G_b}{2(G_b+\kappa_bG_c)}\right.$$
$$\left.\times\left[(\mu_{rb}+\chi_b)H^2V_{ab}^2e^{2i\gamma}\frac{a^6}{b^6}-(\mu_{rc}+\chi_c)H_0^2e^{-2i\gamma}\left(V_{bc}+U_{cb}V_{ab}\frac{H}{H_0}\frac{a^2}{b^2}\right)^2\frac{a^2}{b^2}\right]\right\}\frac{1}{z}-\frac{C_{am}}{2G_a}z=0\quad z\in S_b\cup S_c \tag{A13}$$

where

$$C_{am} = \overline{\phi'_{am}}(0) \tag{A14}$$

It is found from Eq. (47) that T and W are real. By the use of this feature and Eqs. (A6) and (A7), four complex functions $\phi_{am}(z)$, $\omega_{am}(z)$, $\phi_{b0}(z)$ and $\omega_{b0}(z)$ can be solved from Eqs. (A10)–(A13) as

$$\begin{aligned}
\phi_{am}(z) = \mu_0 H_0^2(1+\Lambda_{ab})\Bigg\{ & \frac{1}{1-\Pi_{cb}}\frac{1}{1-\Pi_{ba}}\left[\frac{\chi_b\Pi_{cb}G_b}{\lambda_b+2G_b}\frac{H^2}{H_0^2}\left(1-V_{ab}^2\frac{a^4}{b^4}\right)+\frac{1-\Pi_{cb}}{1+\Lambda_{ab}}\frac{G_a\chi_a\Pi_{ba}U_{ab}^2}{\lambda_a+2G_a}\frac{H^2}{H_0^2}\right.\\
& +(1-\Pi_{cb})(1-\Pi_{ba})(1+\Lambda_{bc})\mu_{rc}^2 T+(\mu_{rb}+\chi_b)V_{ab}\frac{H^2}{H_0^2}\left(\frac{G_b}{G_b+\kappa_b G_c}\frac{a^2}{b^2}-\frac{G_a}{G_a+\kappa_a G_b}\frac{1-\Pi_{cb}}{1+\Lambda_{ab}}\right)\\
& \left.-\frac{G_b(\mu_{rc}+\chi_c)}{G_b+\kappa_b G_c}\left(V_{bc}+U_{cb}V_{ab}\frac{H}{H_0}\frac{a^2}{b^2}\right)\right]z-\left[\frac{\chi_b\Pi_{cb}G_bV_{ab}\mathrm{e}^{-2\mathrm{i}\gamma}}{\lambda_b+2G_b}\frac{H^2}{H_0^2}\frac{a^4}{b^4}+\frac{G_b(\mu_{rb}+\chi_b)V_{ab}^2\mathrm{e}^{-2\mathrm{i}\gamma}}{6(G_b+\kappa_bG_c)}\frac{H^2}{H_0^2}\frac{a^6}{b^6}\right.\\
& \left.-\frac{G_b(\mu_{rc}+\chi_c)}{6(G_b+\kappa_bG_c)}\left(V_{bc}+U_{cb}V_{ab}\frac{H}{H_0}\frac{a^2}{b^2}\right)^2\frac{a^2}{b^2}-\frac{G_a(\mu_{rb}+\chi_b)V_{ab}^2\mathrm{e}^{-2\mathrm{i}\gamma}}{6(1+\Lambda_{ab})(G_a+\kappa_aG_b)}\frac{H^2}{H_0^2}\right]\frac{z^3}{a^2}\Bigg\} \qquad z\in S_a
\end{aligned} \tag{A15}$$

$$\begin{aligned}
\omega_{am}(z) = \mu_0 H_0^2\Bigg\{ & \frac{(1+\Pi_{ab})\chi_bG_b}{\lambda_b+2G_b}\frac{H^2}{H_0^2}\left[\frac{\Pi_{cb}}{1-\Pi_{cb}}\left(1-V_{ab}^2\frac{a^4}{b^4}-3V_{ab}\mathrm{e}^{-2\mathrm{i}\gamma}\frac{a^2}{b^2}\frac{a^2-b^2}{b^2}\right)+V_{ab}\mathrm{e}^{-2\mathrm{i}\gamma}\left(1-\frac{a^2}{b^2}\right)\right]\\
& +(1+\Pi_{ab})(\mu_{rb}+\chi_b)\frac{H^2}{H_0^2}\left[\frac{G_bV_{ab}}{G_b+\kappa_bG_c}\frac{a^2}{b^2}+\frac{G_b\kappa_c\mathrm{e}^{-2\mathrm{i}\gamma}}{2(G_c+\kappa_cG_b)}-\frac{G_bV_{ab}^2\mathrm{e}^{-2\mathrm{i}\gamma}a^4(a^2-b^2)}{2(1-\Pi_{cb})(G_b+\kappa_bG_c)b^6}-\frac{\kappa_bG_a\mathrm{e}^{-2\mathrm{i}\gamma}}{2(1+\Pi_{ab})(G_b+\kappa_bG_a)}\right]\\
& -(1+\Pi_{ab})G_b(\mu_{rc}+\chi_c)\left[\frac{1}{G_b+\kappa_bG_c}\left(V_{bc}+U_{cb}V_{ab}\frac{H}{H_0}\frac{a^2}{b^2}\right)+\frac{\kappa_c\mathrm{e}^{-2\mathrm{i}\gamma}}{2(G_c+\kappa_cG_b)}\right.\\
& \left.-\frac{1}{2(1-\Pi_{cb})(G_b+\kappa_bG_c)}\left(V_{bc}+U_{cb}V_{ab}\frac{H}{H_0}\frac{a^2}{b^2}\right)^2\frac{a^2-b^2}{b^2}\right]+\frac{\chi_cG_c(1+\Pi_{ab})(1+\Pi_{bc})}{\lambda_c+2G_c}\left(V_{bc}+U_{cb}V_{ab}\frac{H}{H_0}\frac{a^2}{b^2}\right)\\
& +\frac{(\mu_{ra}+\chi_a)\kappa_bG_aU_{ab}^2\mathrm{e}^{-2\mathrm{i}\gamma}}{2(G_b+\kappa_bG_a)}\frac{H^2}{H_0^2}+(1+\Pi_{ab})(1+\Pi_{bc})\mu_{rc}^2W\mathrm{e}^{-2\mathrm{i}\gamma}\Bigg\}z\\
& +\frac{1+\Lambda_{ab}}{(1-\Pi_{cb})(1-\Pi_{ba})}\left[\frac{\chi_bG_b\Pi_{cb}}{\lambda_b+2G_b}\frac{H^2}{H_0^2}\left(1-V_{ab}^2\frac{a^4}{b^4}\right)+(\mu_{rb}+\chi_b)V_{ab}\frac{H^2}{H_0^2}\left(\frac{G_b}{G_b+\kappa_bG_c}\frac{a^2}{b^2}-\frac{G_a}{G_a+\kappa_aG_b}\frac{1-\Pi_{cb}}{1+\Lambda_{ab}}\right)\right.\\
& \left.-\frac{G_b(\mu_{rc}+\chi_c)}{G_b+\kappa_bG_c}\left(V_{bc}+U_{cb}V_{ab}\frac{H}{H_0}\frac{a^2}{b^2}\right)+\frac{1-\Pi_{cb}}{1+\Lambda_{ab}}\frac{G_a\chi_a\Pi_{ba}U_{ab}^2}{\lambda_a+2G_a}\frac{H^2}{H_0^2}\right]\frac{a^2}{z} \qquad z\in S_a
\end{aligned} \tag{A16}$$

Notice that the solutions of the complex potential functions $\phi_{b0}(z)$ and $\omega_{b0}(z)$ are shown in Eqs. (53)–(56).

Appendix C. The solving process of $\sum_{n=1}^{\infty}\omega_n(z)$, $\sum_{n=0}^{\infty}\omega_{bn}(z)$, $\sum_{n=1}^{\infty}\phi_{an}(z)$, $\sum_{n=1}^{\infty}\omega_{an}(z)$, $\sum_{n=1}^{\infty}\phi_{cn}(z)$ and $\sum_{n=1}^{\infty}\omega_{cn}(z)$

Adding all the terms with different n in Eq. (86) and using Eqs. (94) and (101) yield

$$\begin{aligned}
\sum_{n=1}^{\infty}\omega_n(z) &= \sum_{n=0}^{\infty}\left[\Lambda_{cb}\overline{\phi_{bn}}\left(\frac{b^2}{z}\right)+\overline{C_{n+1}}\frac{b^2}{z}\right]=\Lambda_{cb}\overline{Q}\frac{z}{b^2}+R\frac{b^2}{z}\\
&=\frac{\Lambda_{cb}\left[3\Pi_{ab}\Pi_{cb}\frac{a^6}{b^6}\frac{a^2-b^2}{a^2}\overline{N_3}+\left(1-\Pi_{cb}\Lambda_{ab}\frac{a^6}{b^6}\right)\overline{K}\right]\frac{a^2}{b^2}z}{\left(1-\Pi_{ab}\Lambda_{cb}\frac{a^2}{b^2}\right)\left(1-\Pi_{cb}\Lambda_{ab}\frac{a^6}{b^6}\right)-3\Pi_{ab}\Pi_{cb}\frac{(a^2-b^2)^2a^2}{b^6}}+\frac{\frac{\Pi_{cb}}{1-\Pi_{cb}}\frac{a^2}{b^2}N_1}{1-\frac{2\Pi_{cb}(\Lambda_{ab}+\Pi_{ba})}{(1-\Pi_{cb})(1-\Pi_{ba})}\frac{a^2}{b^2}}\frac{b^2}{z}
\end{aligned} \tag{A17}$$

$$\begin{aligned}
\sum_{n=0}^{\infty}\omega_{bn}(z) &= N_1\frac{a^2}{z}+N_3\frac{a^4}{z^3}+\sum_{n=1}^{\infty}\left\{\Lambda_{ab}\overline{\phi_n}\left(\frac{a^2}{z}\right)+[(1+\Pi_{ba})\overline{C_{an}}-\overline{C_n}]\frac{a^2}{z}\right\}\\
&=N_1\frac{a^2}{z}+N_3\frac{a^4}{z^3}+\Lambda_{ab}\left(R\frac{a^2}{z}+\overline{P}\frac{a^6}{z^3}\right)+\left[\frac{(1+\Pi_{ba})(1+\Lambda_{ab})}{1-\Pi_{ba}}-1\right]\frac{Ra^2}{z}\\
&=\frac{N_1}{1-\frac{2\Pi_{cb}(\Lambda_{ab}+\Pi_{ba})}{(1-\Pi_{cb})(1-\Pi_{ba})}\frac{a^2}{b^2}}\frac{a^2}{z}+\frac{\left\{1-\Pi_{ab}\frac{a^2}{b^2}\left[\Lambda_{cb}+3\Pi_{cb}\left(\frac{a^2-b^2}{b^2}\right)^2\right]\right\}N_3+\Pi_{cb}\Lambda_{ab}\frac{a^2-b^2}{a^2}\frac{a^6}{b^6}K}{\left(1-\Pi_{ab}\Lambda_{cb}\frac{a^2}{b^2}\right)\left(1-\Pi_{cb}\Lambda_{ab}\frac{a^6}{b^6}\right)-3\Pi_{ab}\Pi_{cb}\frac{(a^2-b^2)^2a^2}{b^6}}\frac{a^4}{z^3}
\end{aligned} \tag{A18}$$

The general expression of the complex potential functions $\phi_{sn}(z)$ and $\omega_{sn}(z)$ with $s = a, b, c$ can be found by replacing the subscript 0 in Eqs. (67), (68) and 1 in Eqs. (78)–(81) with n. Applying these equations gives rise to

$$\begin{aligned}\sum_{n=1}^{\infty}\phi_{an}(z) &= \sum_{n=1}^{\infty}[(1+\Lambda_{ab})\phi_n(z)+\Pi_{ba}C_{an}z] = (1+\Lambda_{ab})(Rz+Pz^3)+\frac{\Pi_{ba}(1+\Lambda_{ab})}{1-\Pi_{ba}}Rz\\ &= \frac{\frac{1+\Lambda_{ab}}{1-\Pi_{ba}}\frac{\Pi_{cb}}{1-\Pi_{cb}}\frac{a^2}{b^2}N_1 z}{1-\frac{2\Pi_{cb}(\Lambda_{ab}+\Pi_{ba})}{(1-\Pi_{cb})(1-\Pi_{ba})}\frac{a^2}{b^2}}+\frac{(1+\Lambda_{ab})\left[\left(1-\Pi_{ab}\Lambda_{cb}\frac{a^2}{b^2}\right)\overline{N_3}+\frac{a^2-b^2}{a^2}\overline{K}\right]\Pi_{cb}\frac{a^6}{b^6}}{\left(1-\Pi_{ab}\Lambda_{cb}\frac{a^2}{b^2}\right)\left(1-\Pi_{cb}\Lambda_{ab}\frac{a^6}{b^6}\right)-3\Pi_{ab}\Pi_{cb}\frac{(a^2-b^2)^2a^2}{b^6}}\frac{z^3}{a^2}\end{aligned} \tag{A19}$$

$$\begin{aligned}\sum_{n=1}^{\infty}\omega_{an}(z) &= \sum_{n=1}^{\infty}\left\{(1+\Pi_{ab})\left[\omega_n(z)+\frac{a^2-b^2}{z}\phi_n'(z)-\overline{C_n}\frac{a^2}{z}\right]+C_{an}\frac{a^2}{z}\right\}\\ &= (1+\Pi_{ab})\left[\Lambda_{cb}\overline{Q}\frac{z}{b^2}+R\frac{b^2}{z}+\frac{a^2-b^2}{z}(R+3Pz^2)-R\frac{a^2}{z}\right]+\frac{1+\Lambda_{ab}}{1-\Pi_{ba}}R\frac{a^2}{z}\\ &= \frac{\frac{1+\Lambda_{ab}}{1-\Pi_{ba}}\frac{\Pi_{cb}}{1-\Pi_{cb}}\frac{a^2}{b^2}N_1}{1-\frac{2\Pi_{cb}(\Lambda_{ab}+\Pi_{ba})}{(1-\Pi_{cb})(1-\Pi_{ba})}\frac{a^2}{b^2}}\frac{a^2}{z}+\frac{(1+\Pi_{ab})\left\{3\Pi_{cb}\frac{a^4(a^2-b^2)}{b^6}\overline{N_3}+\left[\Lambda_{cb}\left(1-\Pi_{cb}\Lambda_{ab}\frac{a^6}{b^6}\right)+3\Pi_{cb}\left(\frac{a^2-b^2}{b^2}\right)^2\right]\frac{a^2}{b^2}\overline{K}\right\}z}{\left(1-\Pi_{ab}\Lambda_{cb}\frac{a^2}{b^2}\right)\left(1-\Pi_{cb}\Lambda_{ab}\frac{a^6}{b^6}\right)-3\Pi_{ab}\Pi_{cb}\frac{(a^2-b^2)^2a^2}{b^6}}\end{aligned} \tag{A20}$$

$$\begin{aligned}\sum_{n=0}^{\infty}\phi_{cn}(z) &= (1+\Lambda_{cb})\sum_{n=0}^{\infty}\phi_{bn}(z) = (1+\Lambda_{cb})\frac{Q}{z}\\ &= \frac{(1+\Lambda_{cb})\left[3\Pi_{ab}\Pi_{cb}\frac{a^6}{b^6}\frac{a^2-b^2}{a^2}N_3+\left(1-\Pi_{cb}\Lambda_{ab}\frac{a^6}{b^6}\right)K\right]}{\left(1-\Pi_{ab}\Lambda_{cb}\frac{a^2}{b^2}\right)\left(1-\Pi_{cb}\Lambda_{ab}\frac{a^6}{b^6}\right)-3\Pi_{ab}\Pi_{cb}\frac{(a^2-b^2)^2a^2}{b^6}}\frac{a^2}{z}\end{aligned} \tag{A21}$$

$$\begin{aligned}\sum_{n=0}^{\infty}\omega_{cn}(z) &= (1+\Pi_{cb})\sum_{n=0}^{\infty}\left[\omega_{bn}(z)+\frac{b^2-a^2}{z}\phi_{bn}'(z)+\overline{C_{n+1}}\frac{b^2}{z}\right]\\ &= (1+\Pi_{cb})\left\{N_1\frac{a^2}{z}+N_3\frac{a^4}{z^3}+\Lambda_{ab}\left(R\frac{a^2}{z}+\overline{P}\frac{a^6}{z^3}\right)+\left[\frac{(1+\Pi_{ba})(1+\Lambda_{ab})}{1-\Pi_{ba}}-1\right]\frac{Ra^2}{z}+\frac{b^2-a^2}{z}\left(-\frac{Q}{z^2}\right)+R\frac{b^2}{z}\right\}\\ &= \frac{(1+\Pi_{cb})\left(1+\frac{\Pi_{cb}}{1-\Pi_{cb}}\right)N_1}{1-\frac{2\Pi_{cb}(\Lambda_{ab}+\Pi_{ba})}{(1-\Pi_{cb})(1-\Pi_{ba})}\frac{a^2}{b^2}}\frac{a^2}{z}+\frac{(1+\Pi_{cb})\left[\left(1-\Pi_{ab}\Lambda_{cb}\frac{a^2}{b^2}\right)N_3+\frac{a^2-b^2}{a^2}K\right]}{\left(1-\Pi_{ab}\Lambda_{cb}\frac{a^2}{b^2}\right)\left(1-\Pi_{cb}\Lambda_{ab}\frac{a^6}{b^6}\right)-3\Pi_{ab}\Pi_{cb}\frac{(a^2-b^2)^2a^2}{b^6}}\frac{a^4}{z^3}\end{aligned} \tag{A22}$$

Notice that the real feature of C_n and the relation $C_{an} = (1+\Lambda_{ab})C_n/(1-\Pi_{ba})$ are used in the derivation of Eqs. (A19) and (A20).

References

[1] S.R. Iyengar, R.S. Alwar, Stress in a layered half-plane, ASCE J. Eng. Mech. Div. 90 (1964) 79–96.
[2] W.T. Chen, Computation of stresses and displacements in a layered elastic medium, Int. J. Eng. Sci. 9 (1971) 775–800.
[3] H. Bufler, Theory of elasticity of a multi-layered medium, J. Elast. 1 (1971) 125–143.
[4] W. Lin, L.M. Keer, Analysis of a vertical crack in a multi-layered medium, J. Eng. Ind. Trans. ASME 56 (1989) 63–69.
[5] S.T. Choi, Y.Y. Earmme, Elastic study on singularities interacting with interfaces using alternating technique: Part II. Isotropic trimaterial, Int. J. Solids Struct. 39 (2002) 1199–1211.
[6] Y. Benveniste, G.J. Dvorak, T. Chen, Stress fields in composite with coated inclusions, Mech. Mater. 7 (1989) 305–317.
[7] H.A. Luo, An edge dislocation in a three-phase composite cylinder model, J. Appl. Mech. Trans. ASME 58 (1991) 75–87.
[8] T. Honein, E. Honein, G. Herrmann, Circularly cylindrical and plane layered media in anti-plane elastostatics, J. Appl. Mech. Trans. ASME 61 (1994) 243–249.
[9] C.K. Chao, F.M. Chen, M.H. Shen, Circularly cylindrical layered media in plane elasticity, Int. J. Solids Struct. 43 (2006) 4739–4756.
[10] G.A. Maugin, M. Epstein, C. Trimarco, Theory of elastic inhomogeneities in electromagnetic materials, Int. J. Eng. Sci. 30 (1992) 1441–1449.
[11] C.B. Lin, On a bounded elliptic elastic inclusion in plane magnetoelasticity, Int. J. Solids Struct. 40 (2003) 1547–1565.
[12] C.B. Lin, S.C. Chen, Magnetoelastic stresses in a circular shell subject to a point magnetic source, Int. J. Appl. Electromagn. Mech. 18 (2003) 199–216.
[13] S.C. Chen, C.B. Lin, On multiple circular inclusions in plane magnetoelasticity, Int. J. Solids Struct. 43 (2006) 6243–6260.
[14] A.H. England, Complex Variable Methods in Elasticity, Wiley Interscience, New York, 1971.
[15] C.B. Lin, S.C. Chen, J.L. Lee, Explicit solutions of magnetoelastic fields in a soft ferromagnetic solid with curvilinear cracks, Eng. Fract. Mech. 76 (2009) 1846–1865.
[16] J. Dundurs, Concentrated force in an elastically embedded disk, J. Appl. Mech. Trans. ASME 30 (1969) 568–570.